Chapter 5

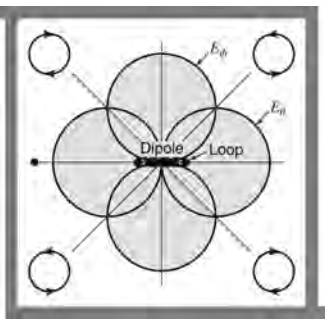

Point Sources and Their Arrays

Topics in this chapter include:

- Point source radiators
- Power patterns
- Isotropic sources
- Radiation intensity
- Examples of power patterns field patterns
- Field patterns
- Phase patterns
- Arrays of two point sources
- Pattern multiplication
- Pattern synthesis
- Non-isotropic dissimilar sources
- Linear arrays of n point sources
- Null directions and beam widths
- Non uniform amplitude distributions
- Dolph-Tschebycheff (D-T) or optimum distribution
- D-T distribution for an array of 8-point sources
- A comparison of amplitude distributions
- Continuous arrays
- Huygen's principle
- Diffraction by flat sheet
- Rectangular broadside arrays

5–1 Introduction

In chap. 2 an antenna was treated as an aperture. In this chapter an antenna is first considered as a point source and later the concept is extend to the formation of arrays of point source. This approach is of great value since **the pattern of any antenna can be regarded as produced by an array of point sources**. Further the initial discussion relating to arrays is confined to isotropic point sources, which may represent different kinds of antennas. Later the discussion is extended to encompass more general case of non-uniform distribution.

With the information of this chapter and the computer programs on the book's website, an arrays producing almost any desired patterns may be designed.

5–2 Point Source Defined

At a sufficient distance in the far field of an antenna, the radiated fields of the antenna are transverse and the power flow or Poynting vector (Wm^{-2}) is radial as at the point O at a distance R on the observation circle in Fig. 5−1. It is convenient in many analyses to assume that the fields of the antenna are everywhere of this type. In fact, we may assume, by extrapolating inward along the radii of the circle, that the waves originate at a fictitious volumeless emitter, or *point source*, at the center O of the observation circle. The actual field variation near the antenna, or "near field," is ignored, and we describe the source of the waves only in terms

of the "far field" it produces. Provided that our observations are made at a sufficient distance, any antenna, regardless of its size or complexity, can be represented in this way by a single point source.

Instead of making field measurements around the observation circle with the antenna fixed, the equivalent effect may be obtained by making the measurements at a fixed point Q on the circle and rotating the antenna around the center O. This is usually the more convenient procedure if the antenna is small.

In Fig. 5−1*a*, the center O of the antenna coincides with the center of the observation circle. If the center of the antenna is displaced from O, even to the extent that O lies outside the antenna as in Fig. 5−1*b*, the distance d between the two centers has a negligible effect on the field patterns at the observation circle, provided $R \gg d$, $R \gg b$, and $R \gg \lambda$. However, the phase patterns will generally differ, depending on d. If $d = 0$, the phase shift around the observation circle is usually a minimum. As d is increased, the observed phase shift becomes larger.

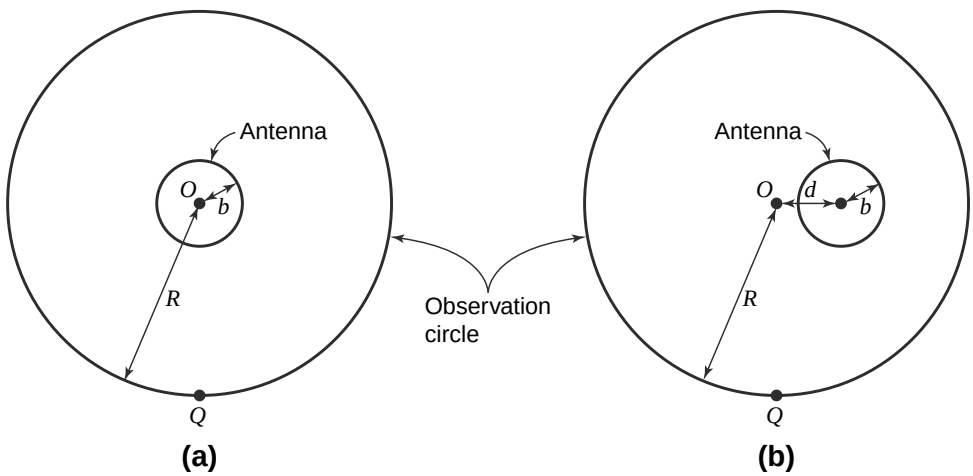

Figure 5–1 Antenna and observation circle.

As discussed in Sec. 2−3, a complete description of the far field of a source requires three patterns: two patterns of orthogonal field components as a function of angle [$E_\theta\ (\theta, \phi)$ and $E_\phi(\theta, \phi)$] and one pattern of the phase difference of these fields as a function of angle [$\delta\ (\theta, \phi)$]. For many purposes, however, such a complete knowledge is not necessary. It may suffice to specify only the variation with angle of the power density or Poynting vector magnitude (power per unit area) from the antenna [$S_r\ (\theta, \phi)$]. In this case the vector nature of the field is disregarded, and the radiation is treated as a scalar quantity. This is done in Sec. 5−3. The vector nature of the field is recognized later in the discussion on the magnitude of the field components. Although the cases considered as examples in this chapter are hypothetical, they could be approximated by actual antennas.

5–3 Power Patterns

Let a transmitting antenna in free space be represented by a point-source radiator located at the origin of the coordinates in Fig. 5−2 (see also Fig. 2−5). The radiated energy streams from the source in radial lines. The time rate of energy flow per unit area is the *Poynting vector*, or *power density* (watts per square meter). For a point source (or in the far field of any antenna), the Poynting vector **S** has only a radial component S_r with no components in either the θ or ϕ directions ($S_\theta = S_\phi = 0$). Thus, the magnitude of the Poynting vector, or power density, is equal to the radial component ($|\mathrm{S}| = S_r$).

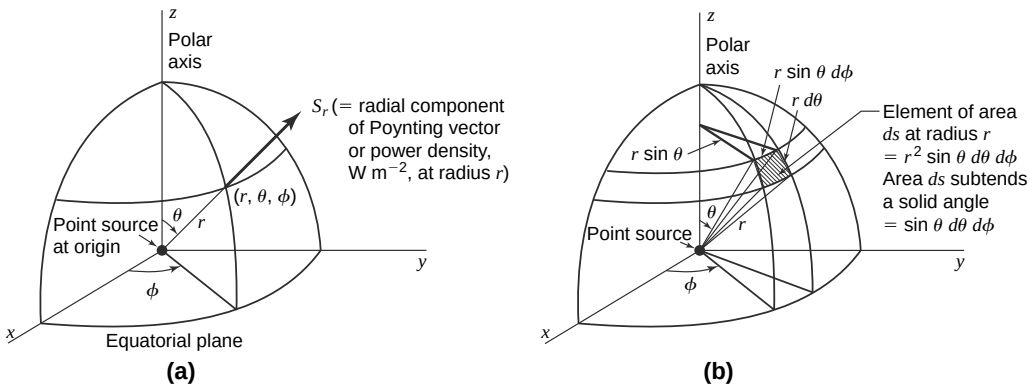

Figure 5–2 Spherical coordinates for a point source of radiation in free space.

A source that radiates energy uniformly in all directions is an *isotropic source.* For such a source the radial component S_r of the Poynting vector is independent of θ and ϕ. A graph of S_r at a constant radius as a function of angle is a Poynting vector, or power-density, pattern, but is usually called a *power pattern.* The three-dimensional power pattern for an isotropic source is a sphere. In two dimensions the pattern is a circle (a cross section through the sphere), as suggested in Fig. 5−3.

Although the isotropic source is convenient in theory, it is not a physically realizable type. Even the simplest antennas have directional properties, i.e., they radiate more energy in some directions than in others. In contrast to the isotropic source, they might be called *anisotropic* sources. As an example, the power pattern of such a source is shown in Fig. 5−4*a* where S_{rm} is the maximum value of S_r.

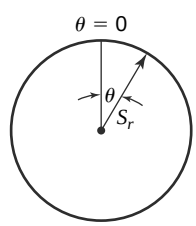

Figure 5–3 Polar power pattern of isotropic source.

If S_r is expressed in watts per square meter, the graph is an *absolute power pattern.* On the other hand, if S_r is expressed in terms of its value in some reference direction, the graph is a *relative power pattern.* It is customary to take the reference direction such that S_r is a maximum. Thus, the pattern radius for relative power is S_r / S_{rm} where S_{rm} is the maximum value of S_r. The maximum value of the relative power pattern is unity, as shown in Fig. 5−4*b*. A pattern with a maximum of unity is also called a *normalized pattern.*

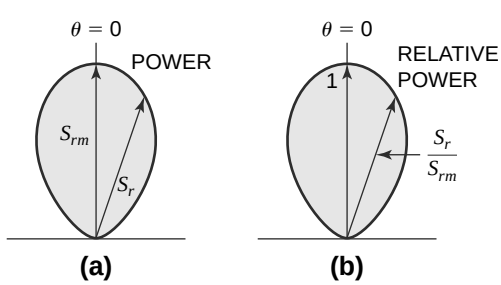

Figure 5–4 (*a*) Power pattern and (*b*) relative power pattern for same source. Both patterns have the same shape. The relative power pattern is normalized to a maximum of unity (1).

5–4 A Power Theorem[1] and its Application to an Isotropic Source

If the Poynting vector is known at all points on a sphere of radius r from a point source in a lossless medium, *the total power radiated by the source is the integral over the surface of the sphere of the radial component S_r of the average Poynting vector.* Thus,

$$P = \oiint S \cdot ds = \oiint S_r \, ds \tag{1}$$

where

P = power radiated, W
S_r = radial component of average Poynting vector, W m^{-2}
ds = infinitesimal element of area of sphere (see Fig. 3−2*b*)
$= r^2 \sin\theta \, d\theta \, d\phi$, m^2

For an *isotropic source*, S_r is independent of θ and ϕ so

$$P = S_r \oiint ds = S_r \times 4\pi r^2 \qquad \text{(W)} \tag{2}$$

and

$$S_r = \frac{P}{4\pi r^2} \qquad \text{(W m}^{-2}\text{)} \tag{3}$$

Equation (3) indicates that the magnitude of the Poynting vector varies inversely as the square of the distance from a point-source radiator. This is a statement of the well-known law for the variation of power per unit area as a function of the distance.

5–5 Radiation Intensity

As discussed in Sec. 2−5, the radiation intensity **U** is expressed in watts per unit solid angle (W sr^{-1}). The radiation intensity is independent of radius. It is power per steradian. From (5−4−3) we have

$$r^2 S_r = P/4\pi = U \qquad \text{(W/sr)} \tag{1}$$

Thus, the power theorem may be restated as follows:

The total power radiated is given by the integral of the radiation intensity over a solid angle of 4π steradians.

As already mentioned in Sec. 2−5, power patterns can be expressed in terms of either the Poynting vector (power density) or the radiation intensity. A power pattern in terms of U is the same as in Fig. 5−4*a* with the maximum Poynting vector (S_m) replaced by the maximum radiation intensity (U_m) and the Poynting vector

---

[1]This theorem is a special case of a more general relation for the complex power flow through any closed surface as given by

$$P = \frac{1}{2} \oiint (\mathbf{E} \times \mathbf{H}^*) \cdot ds \tag{1}$$

where P is the total complex power flow and **E** and $\mathbf{H}^*$ are complex vectors representing the electric and magnetic fields, $\mathbf{H}^*$ being the complex conjugate of **H**. The average Poynting vector is

$$S = \frac{1}{2} \operatorname{Re}(\mathbf{E} \times \mathbf{H}^*) \tag{2}$$

Now the power flow in the far field is entirely real; hence, taking the real part of (1) and substituting (2), we obtain the special case of (3).

as a function of $r(S_r)$ replaced by the radiation intensity as a function of $r(U_r)$. The maximum value of U_m is in the $\theta = 0$ direction. Relative Poynting vector (or power density) and relative radiation intensity patterns are identical.

Applying (1) to an isotropic source gives

$$P = 4\pi U_0 \qquad \text{(W)}$$

where U_0 = radiation intensity of isotropic source, W sr^{-1}.

5–6 Examples of Power Patterns

EXAMPLE 5–6.1 Source with Unidirectional Cosine Power Pattern

A source has a cosine radiation-intensity pattern, that is,

$$U = U_m \cos\theta \tag{1}$$

where U_m = maximum radiation intensity

The radiation intensity U has a value only in the upper hemisphere ($0 \le \theta \le \pi/2$ and $0 \le \phi \le 2\pi$) and is zero in the lower hemisphere. The radiation intensity is a maximum at $\theta = 0$. The pattern is shown in Fig. 5−5. The space pattern is a figure of revolution of this circle around the polar axis. Find the directivity.

To find the total power radiated by the cosine source, we apply (5−4−1) and integrate only over the upper hemisphere. Thus

$$P = \int_0^{2\pi} \int_0^{\pi/2} U_m \cos\theta \sin\theta \, d\theta \, d\phi = \pi U_m \tag{2}$$

If the power radiated by the unidirectional cosine source is the same as for an isotropic source, then (2) and (1) in Sec. 5−5 may be set equal, yielding

$$\pi U_m = 4\pi U_0$$

or

$$\text{Directivity} = \frac{U_m}{U_0} = 4 = D \qquad \textit{Ans} \tag{3}$$

Thus, the maximum radiation intensity U_m of the unidirectional cosine source (in the direction $\theta = 0$) is 4 times the radiation intensity U_0 from an isotropic source radiating the same total power. The power patterns for the two sources are compared in Fig. 5−6 for the same total power radiated by each.

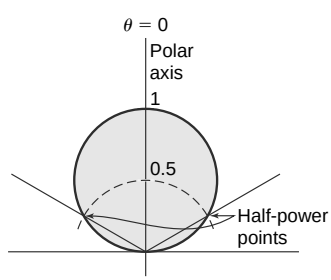

Figure 5–5 Unidirectional cosine power pattern.

EXAMPLE 5–6.2 Source with Bidirectional Cosine Power Pattern

A source has a cosine power pattern that is bidirectional. Find the directivity. With radiation in two hemispheres instead of one; the maximum radiation intensity is half its value in Example 5−6.1. Thus, from (3),

$$D = 4/2 = 2 \qquad \textit{Ans.}$$

EXAMPLE 5–6.3 Source with Sine (Doughnut) Power Pattern

A source has a radiation intensity pattern given by

$$U = U_m \sin\theta \tag{4}$$

The pattern is shown in Fig. 5−6. The space pattern is a figure-of-revolution of this pattern around the polar axis and has the form of a doughnut. Find D.

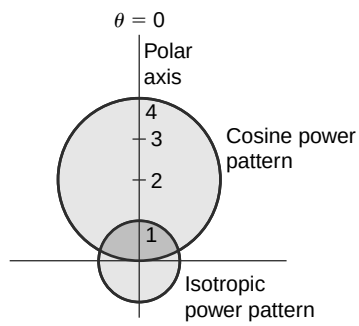

Figure 5–6
Power patterns of cosine and isotropic sources.

Solution

Applying (5−4−3) the total power radiated is

$$P = U_m \int_0^{2\pi} \int_0^{\pi} \sin^2\theta \, d\theta \, d\phi = \pi^2 U_m \tag{5}$$

If the power radiated by this source is the same as for an isotropic source taken as reference, we have

$$\pi^2 U_m = 4\pi U_0 \tag{6}$$

and

$$\text{Directivity} = \frac{U_m}{U_0} = \frac{4}{\pi} = 1.27 = D \qquad \textit{Ans.} \tag{7}$$

EXAMPLE 5–6.4 Source with Sine-Squared (Doughnut) Power Pattern

A source has a sine-squared radiation-intensity power pattern. The radiation-intensity pattern is given by

$$U = U_m \sin^2\theta \tag{8}$$

The power pattern is shown in Fig. 5−7*a*. This type of pattern is of considerable interest because it is the pattern produced by a short dipole coincident with the polar ($\theta = 0$) axis in Fig. 5−7*a*. Applying (5−4−3), the total power radiated is

$$P = U_m \int_0^{2\pi} \int_0^{\pi} \sin^3\theta \, d\theta \, d\phi = \frac{8}{3}\pi U_m \tag{9}$$

If P is the same as for the isotropic source,

$$\frac{8}{3}\pi U_m = 4\pi U_0$$

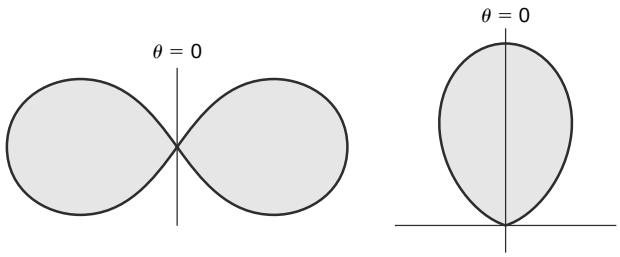

Figure 5–7 (*a*) Sine-squared power pattern and (*b*) unidirectional cosine-squared power pattern.

and

$$\text{Directivity} = \frac{U_m}{U_0} = \frac{3}{2} = 1.5 = D \qquad \textit{Ans.} \tag{10}$$

EXAMPLE 5–6.5 Source with Unidirectional Cosine-Squared Power Pattern

A source with a unidirectional cosine-squared radiation-intensity pattern is given by

$$U = U_m \cos^2 \theta \tag{11}$$

The radiation intensity has a value only in the upper hemisphere as in Fig. 5−7*b*. The three-dimensional or space pattern is a figure-of-revolution of this pattern around the polar ($\theta = 0$) axis. Find the directivity.

Solution

The total power radiated is

$$P = U_m \int_0^{2\pi} \int_0^{\pi/2} \cos^2 \theta \sin \theta \, d\theta \, d\phi = \frac{2}{3} \pi U_m \tag{12}$$

If P is the same as radiated by an isotropic source,

$$\frac{2}{3} \pi U_m = 4\pi U_0$$

and

$$\text{Directivity} = \frac{U_m}{U_0} = 6 = D \qquad \textit{Ans.} \tag{13}$$

Thus, the maximum power per unit solid angle (at $\theta = 0$) from the source with the cosine-squared power pattern is six times the power per unit solid angle from an isotropic source radiating the same power.

Directivities are summarized in Table 5−1.

Example 5−6.6 provides some valuable insights into the effect minor lobes have on directivity or gain. Without minor lobes the gain of this antenna would be 91.4 or 19.6 dBi as compared to a gain of 18.0 or 12.6 dBi with minor lobes. The minor lobes have large beam or solid angles because they extend 360° in the azimuth or ϕ direction at large sin θ values (θ near 90°). The main lobe, on the other hand, is at small θ angles so the $P_n(\theta)$ sin θ product is small, in fact, zero at $\theta = 0°$.

Table 5–1 Directivities of the Point Source Patterns in Examples 5−6.1 to 5−6.5.

Pattern	Directivity
Unidirectional cosine	4
Bidirectional cosine	2
Sine doughnut	1.27
Sine-squared doughnut	1.5
Unidirectional cosine squared	6

EXAMPLE 5–6.6 Pencil Beam with Minor Lobes

As shown in Fig. 5−8, the pattern has pencil beam (symmetrical around the $\theta = 0$ axis) with a main-lobe HPBW of approximately 22° and four minor lobes. Find the directivity.

Solution

The directivity is given by

$$D = \frac{4\pi}{\int_0^{2\pi}\int_0^{\pi} P_n(\theta)\sin\theta\, d\theta\, d\phi} \tag{14}$$

where the denominator equals the total beam area Ω_A.

Since the pattern is symmetrical (no variation with ϕ), the integral with respect to ϕ yields 2π and (14) reduces to

$$D = \frac{4\pi}{2\pi\int_0^{\pi} P_n(\theta)\sin\theta\, d\theta} \tag{15}$$

We have only the pattern graph available (no analytical expression), so let us divide the pattern (Fig. 5−8) into 36 steps of 5° each. The approximate value of the integral in the first ($m = 1$) 5° section ($= \pi/36$ rad) is given by

$$\frac{\pi}{36} P_n(\theta_1)_{\text{av}} \sin\theta_1 = \frac{\pi}{36}\frac{1.0 + 0.93}{2}\sin 2.5° \tag{16}$$

and the approximate directivity is then given by the summation of all 36 sections or by

$$D \simeq \frac{4\pi}{2\pi(\pi/36)\sum_{m=1}^{m=36} P_n(\theta_m)_{\text{av}}\sin\theta_m} \tag{17}$$

Completing the summation, we obtain

$$D = \frac{4\pi}{\Omega_A} \simeq \frac{4\pi}{2\pi(\pi/36)(0.25 + 0.37 + 0.46 + 0.12 + 0.07)} = \frac{72}{1.27\pi} = 18.0 \tag{18}$$

Main lobe; First minor lobe; Second minor lobe; Third minor lobe; Fourth minor lobe (back lobe)

or $D \simeq 12.6$ dBi

It is noteworthy that the second minor lobe contributes most to the total beam area, the first minor lobe almost as much, and the main lobe less than either. Thus, the directivity is greatly affected by the minor

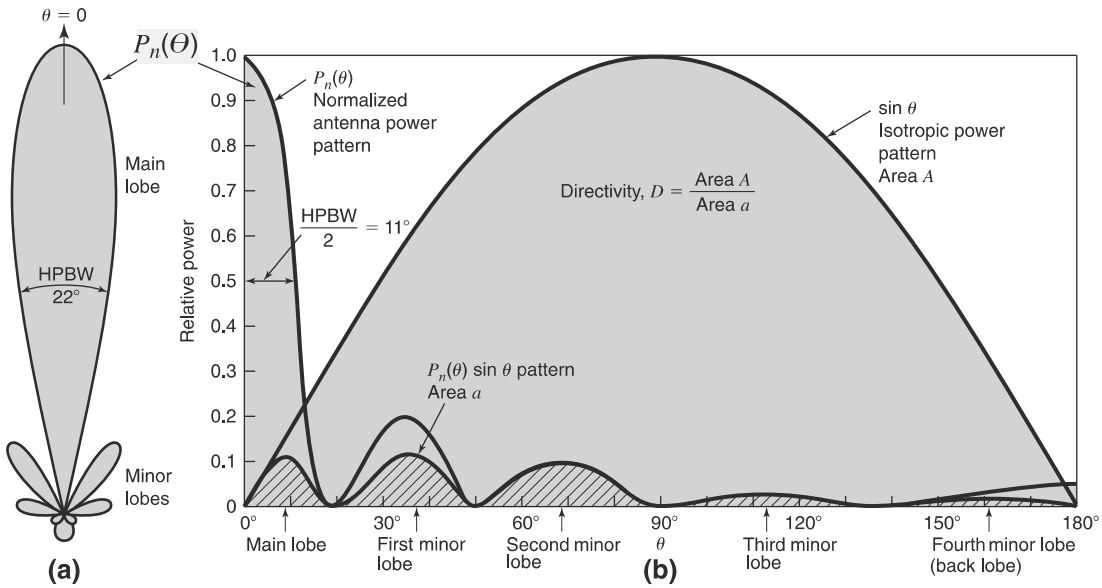

Figure 5–8 Power patterns of beam antenna in polar plot at (*a*) and in rectangular plot at (*b*). The large shaded area A of (*b*) is for an isotropic source while the antenna area a appears as a series of small areas. The directivity $D = A / a$

lobes, which is a common situation with actual antennas. For this antenna pattern the beam efficiency is given by

$$\varepsilon_M = \frac{0.25}{1.27} = 0.20 \tag{19}$$

If the second minor lobe were eliminated, the directivity would increase to 14.5 dBi (up 1.9 dB) and if both first and second minor lobes were eliminated, the directivity would increase to 17.1 dBi (up 4.5 dB).

The directivity obtained in Example 5−6.6 is approximate. By sufficiently reducing the step size (5° in the example), the summation can be made as precise as the available data will allow. Computation of this numerical integration can be facilitated by using a computer.

The half-power beamwidth of the pattern in the example is about 22°. Taking $k_p = 1$ and ε_M as in (19), the approximate directivity is then

$$D \simeq \frac{41{,}000\varepsilon_M}{k_p \times \text{HPBW}^2} = \frac{41{,}000 \times 0.2}{(22°)^2} = 16.9 \text{ or } 12.3 \text{ dBi} \tag{20}$$

which is 0.3 dB less than obtained by the 36-step summation.

The beam area of an isotropic source equals 4π steradians. In Fig. 5−8*b* this corresponds to the area A under the sin θ curve. The beam area of the source in Example 5−6.6 corresponds to the area a under the $P_n(\theta) \sin\theta$ curve. Thus, the directivity is simply A/a or the ratio of the area of the isotropic source to the area of the source being measured. Hence,

$$D = \frac{4\pi}{\Omega_A} = \frac{A}{a} \tag{21}$$

If the areas A and a are cut from a lead sheet of uniform thickness, the directivity equals the ratio of the weight of A to the weight of a.

5–7 Field Patterns

The discussion in the preceding sections is based on considerations of power. This has afforded a simplicity of analysis, since the power flow from a point source has only a radial component which can be considered as a scalar quantity. To describe the field of a point source more completely, we need to consider the electric field **E** and/or the magnetic field **H** (both vectors). For point sources we deal entirely with *far fields* so **E** and **H** are both entirely transverse to the wave direction, are perpendicular to each other, are in-phase, and are related in magnitude by the intrinsic impedance of the medium ($\mathbf{E}/\mathbf{H} = Z = 377\ \Omega$ for free space). For our purposes it suffices to consider only one field vector, and we arbitrarily choose the electric field **E**.

Since the Poynting vector around a point source is everywhere radial, it follows that the electric field is entirely transverse, having only E_θ and E_ϕ components. The relation of the radial component S_r of the Poynting vector and the electric field components is illustrated by the spherical coordinate diagram of Fig. 5−9. The conditions characterizing the far field are then:

1. Poynting vector radial (S_r component only)
2. Electric field transverse (E_θ and E_ϕ components only)

The Poynting vector and the electric field at a point of the far field are related in the same manner as they are in a plane wave, since, if r is sufficiently large, a small section of the spherical wave front may be considered as a plane.

The relation between the average Poynting vector and the electric field at a point of the far field is

$$S_r = \frac{1}{2}\frac{E^2}{Z} \tag{1}$$

where Z_0 = intrinsic impedance of medium and

$$E = \sqrt{E_\theta^2 + E_\phi^2} \tag{2}$$

where

E = amplitude of total electric field intensity
E_θ = amplitude of θ component
E_ϕ = amplitude of ϕ component

The field may be elliptically, linearly or circularly polarized.

If the field components are rms values, rather than amplitudes, the Poynting vector is twice that given in (1).

A pattern showing the variation of the electric field intensity at a constant radius r as a function of angle (θ, ϕ) is called a *field pattern*. In presenting information concerning the far field of an antenna, it is customary to give the field patterns for the two components, E_θ and E_ϕ, of the electric field since the total electric field **E** can be obtained from the components by (2), but the components cannot be obtained from a knowledge of only **E**.

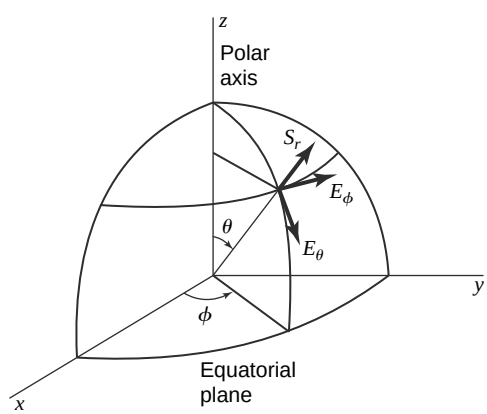

Figure 5–9 Relation of the Poynting vector S and the two electric field components of the far field.

When the field intensity is expressed in volts per meter, it is an *absolute field pattern*.[1] On the other hand, if the field intensity is expressed in units relative to its value in some reference direction, it is a *relative field pattern*. The reference direction is usually taken in the direction of maximum field intensity. The relative pattern of the E_θ component is then given by

$$\frac{E_\theta}{E_{\theta m}} \tag{3}$$

and the relative pattern of the E_ϕ component is given by

$$\frac{E_\phi}{E_{\phi m}} \tag{4}$$

where

$E_{\theta m}$ = maximum value of E_θ
$E_{\phi m}$ = maximum value of E_ϕ

The magnitudes of both the electric field components, E_θ and E_ϕ, of the far field vary inversely as the distance from the source. However, they may be different functions, F_1 and F_2, of the angular coordinates, θ and ϕ. Thus, in general,

$$E_\theta = \frac{1}{r}F_1(\theta, \phi) \tag{5}$$

$$E_\phi = \frac{1}{r}F_2(\theta, \phi) \tag{6}$$

Since $S_{rm} = E_m^2/2Z$, where E_m is the maximum value of E, it follows on dividing this into (1) that the relative total power pattern is equal to the square of the relative total field pattern. Thus,

$$P_n = \frac{S_r}{S_{rm}} = \frac{U}{U_m} = \left(\frac{E}{E_m}\right)^2 \tag{7}$$

EXAMPLE 5–7.1 Source with Cosine Field Pattern

An antenna's far field has only an E_ϕ component in the equatorial plane, the E_θ component being zero in this plane. The relative equatorial-plane pattern of the E_ϕ component (that is, E_ϕ as a function of ϕ for $\theta = 90°$) is given by

$$\frac{E_\phi}{E_{\phi m}} = \cos\phi \tag{8}$$

This pattern is illustrated at the left of Fig. 5−10. The length of the radius vector in the diagram is proportional to E_ϕ. A pattern of this form could be produced by a short dipole coincident with the y axis. Find D.

The relative (normalized) power pattern in the equatorial plane is equal to the square of the relative field pattern. Thus

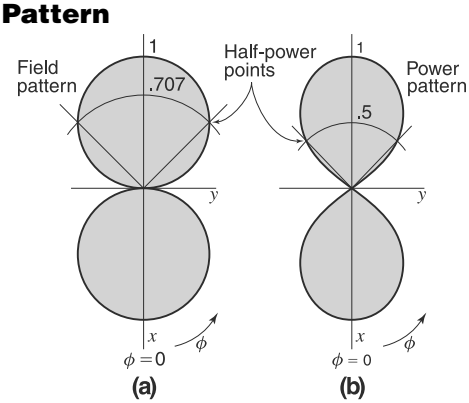

Figure 5–10 (*a*) Relative E_ϕ pattern of Example 5−7.1 and (*b*) the relative power pattern.

[1]The magnitude depends on the radius, varying inversely as the distance ($E \propto 1/r$).

$$P_n = \frac{S_r}{S_{rm}} = \frac{U}{U_m} = \left(\frac{E_\phi}{E_{\phi m}}\right)^2 \tag{9}$$

and substituting (8) into (9) we have

$$P_n = \cos^2 \phi$$

This pattern is illustrated at the right of Fig. 5−10.

EXAMPLE 5–7.2 Source with Sine Field Pattern

An antenna has a far field that has only an E_θ component in the equatorial plane, the E_ϕ component being zero in this plane. Assume that the relative equatorial-plane pattern of the E_θ component (that is, E_θ as a function of ϕ for $\theta = 90°$) for this antenna is given by

$$\frac{E_\theta}{E_{\theta m}} = \sin \phi \tag{10}$$

This pattern is illustrated by Fig. 5−11*a* and could be produced by a small loop antenna, the axis of the loop coincident with the x axis. Find D.

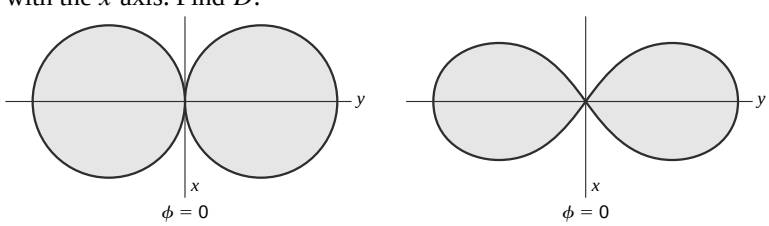

Figure 5–11 (*a*) Relative E_θ pattern of Example 5−7.2 and (*b*) the relative power pattern.

The relative (normalized) power pattern in the equatorial plane is

$$P_n = \sin^2 \phi \tag{11}$$

This pattern is shown by Fig. 5−11.

EXAMPLE 5–7.3 Short Dipole and Loop Patterns

An antenna's far field has both E_θ and E_ϕ components in the equatorial plane ($\theta = 90°$). Suppose that this antenna is a composite of the two antennas we have just considered in Examples 5−7.1 and 5−7.2 and that equal power is radiated by each antenna. If both patterns are of identical shape in three dimensions as well as in the xy plane, as from a short dipole and a small loop, it then follows that at a radius r from the composite antenna, $E_{\theta m} = E_{\phi m}$. The individual patterns for the E_θ and E_ϕ components as given by (10) and (8) may then be shown to the same scale by one diagram, as in Fig. 5−12*a*. The relative pattern of the total field E is

$$\frac{E}{E_m} = \sqrt{\sin^2 \phi + \cos^2 \phi} = 1 \tag{12}$$

which is a circle as indicated by the dashed line in Fig. 5−12*a*. Find D.

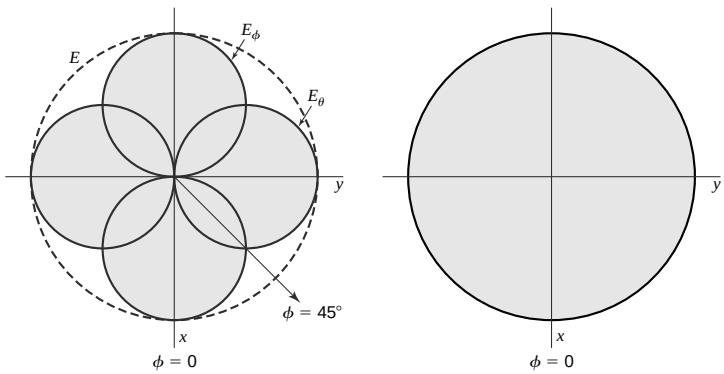

Figure 5–12 (*a*) Relative patterns of E_θ and E_ϕ components of the electric field and the total field E (dashed) of the antenna of Example 5–7.3. (*b*) Relative total power pattern.

The relative pattern in the equatorial plane for the total power is therefore a circle of radius unity as illustrated by Fig. 5−12*b*.

We note in Fig. 5−12*a* that at $\phi = 45°$ the magnitudes of the two field components, E_θ and E_ϕ, are equal. Depending on the time phase between E_θ and E_ϕ, the field in this direction could be plane, elliptically or circularly polarized, but regardless of phase the power is the same. To determine the type of polarization requires that the phase angle between E_θ and E_ϕ be known. This is discussed in the next section.

5–8 Phase Patterns

Assuming that the field varies harmonically with time and that the frequency is known, the far field in all directions from a source may be completely specified by a knowledge of the following four quantities:

1. Amplitude of the polar component E_θ of the electric field as a function of r, θ, and ϕ
2. Amplitude of the azimuthal component E_ϕ of the electric field as a function of r, θ, and ϕ
3. Phase lag δ of E_ϕ behind E_θ as a function of θ and ϕ
4. Phase lag η of either field component behind its value at a reference point as a function of r, θ, and ϕ

Since we regard the field of a point source as a far field everywhere, the above four quantities can be considered as those required for a complete knowledge of the field of a point source.

If the amplitudes of the field components are known at a particular radius from a point source in free space, their amplitudes at all distances are known from the inverse-distance law. Thus, it is usually sufficient to specify E_θ and E_ϕ as a function only of θ and ϕ as, for example, by a set of field patterns.

Figure 5−13 shows the pattern of Fig. 2−3 in three-dimensional, polar and decibel displays. Note that the polarity of the lobes alternate (+ and −). Thus, when the magnitude of the field of one lobe (+) and the adjacent lobe (−) are equal, the total field goes to zero, producing a null.

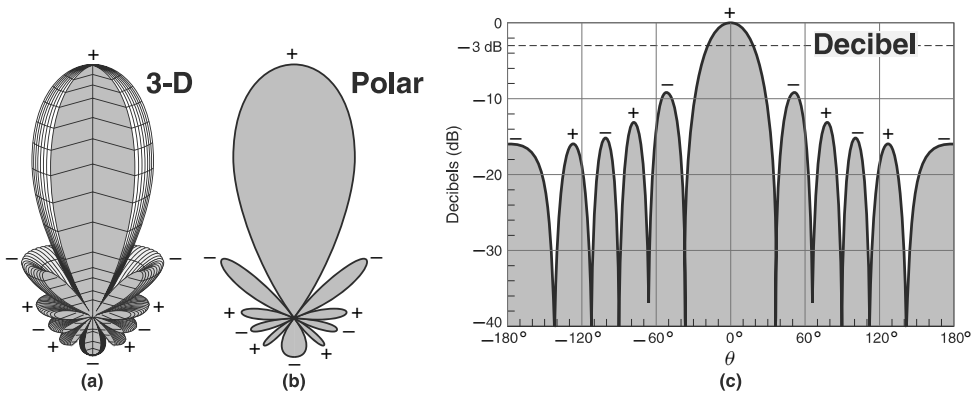

Figure 5–13 Three-dimensional field pattern at (*a*), polar pattern at (*b*), and decibel pattern at (*c*) showing alternate phasing (+ and −) of pattern lobes.

EXAMPLE 5–8.1 Field of Dipole and Loop in Phase Quadrature

A short dipole is situated inside a small loop as in Fig. 5−14. The magnitude of the fields of both dipole and loop are equal. If the dipole and loop are fed in quadrature or 90° phasing, what are the fields that are observed as a function of azimuth in the plane of the page?

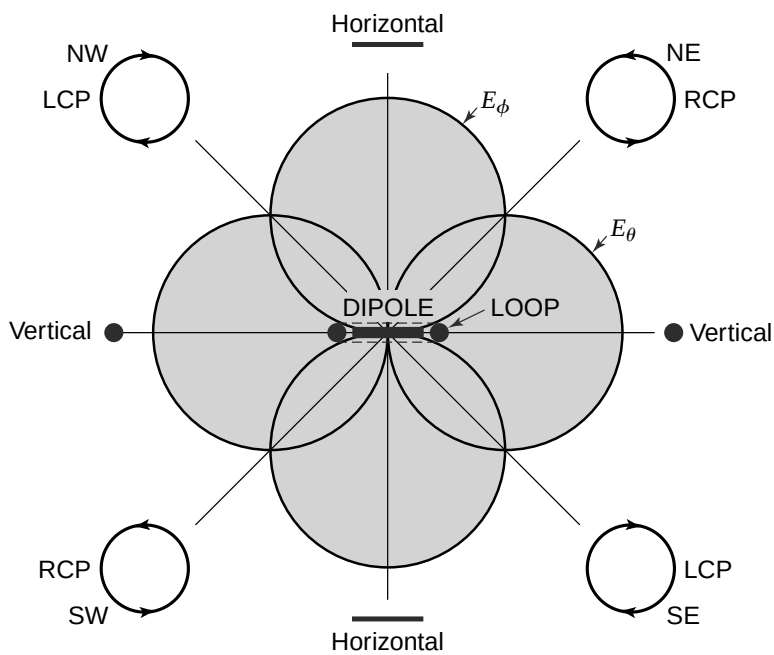

Figure 5–14 Fields of short dipole and small loop of equal magnitude and in phase quadrature (90°).

■ **Solution**

The fields north and south are horizontally polarized (in the plane of the page). The fields east and west are vertically polarized. At 45° or NE the field is right circularly polarized (RCP). At 135° or SE the field is left circularly polarized (LCP). At 225° or SW the field is again right circularly polarized. Finally, at 315° or NW the field is again left circularly polarized. At intermediate angles the field is elliptically polarized.

5–9 Arrays of Two Isotropic Point Sources

Let us introduce the subject of arrays of point sources by considering the simplest situation, namely, that of two isotropic point sources. As illustrations, five cases involving two isotropic point sources are discussed.

Case 1. Two Isotropic Point Sources of Same Amplitude and Phase

The first case we shall analyze is that of two isotropic point sources having equal amplitudes and oscillating in the same phase. Let the two point sources, 1 and 2, be separated by a distance d and located symmetrically with respect to the origin of the coordinates as shown in Fig. 5−15*a*. The angle ϕ is measured counterclockwise

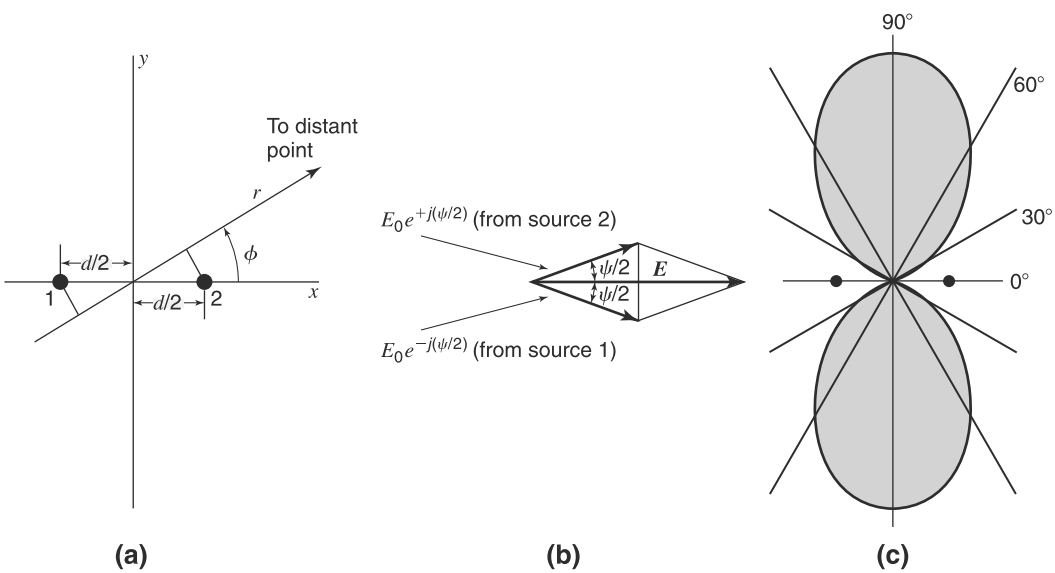

Figure 5–15 (*a*) Relation to coordinate system of two isotropic point sources separated by a distance *d*. (*b*) Vector addition of the fields from two isotropic point sources of equal amplitude and same phase located as in (*a*). (*c*) Field pattern of two isotropic point sources of equal amplitude and same phase located as in (*a*) for the case where the separation $d = \lambda/2$.

from the positive x axis. The origin of the coordinates is taken as the reference for phase. Then at a distant point in the direction ϕ the field from source 1 is retarded by $\frac{1}{2}d_r \cos\phi$, while the field from source 2 is advanced by $\frac{1}{2}d_r \cos\phi$, where d_r is the distance between the sources expressed in radians; that is,

$$d_r = \frac{2\pi d}{\lambda} = \beta d$$

The total field at a large distance r in the direction ϕ is then

$$E = E_0 e^{-j\psi/2} + E_0 e^{+j\psi/2} \tag{1}$$

where $\psi = d_r \cos\phi$ and the amplitude of the field components at the distance r is given by E_0.

The first term in (1) is the component of the field due to source 1 and the second term the component due to source 2. Equation (1) may be rewritten

$$E = 2E_0 \frac{e^{+j\psi/2} + e^{-j\psi/2}}{2} \tag{2}$$

which by a trigonometric identity is

$$E = 2E_0 \cos\frac{\psi}{2} = 2E_0 \cos\left(\frac{d_r}{2}\cos\phi\right) \tag{3}$$

This result may also be obtained with the aid of the vector diagram[1] shown in Fig. 5−15*b*, from which (3) follows directly. We note in Fig. 5−15*b* that the phase of the total field E does not change as a function of ψ. To normalize (3), that is, make its maximum value unity, set $2E_0 = 1$. Suppose further that d is $\lambda/2$. Then $d_r = \pi$. Introducing these conditions into (3) gives

$$E = \cos\left(\frac{\pi}{2}\cos\phi\right) \tag{4}$$

The field pattern of E versus ϕ as expressed by (4) is presented in Fig. 5−15*c*. The pattern is a bidirectional figure-of-eight with maxima along the y axis. The space pattern is doughnut-shaped, being a figure-of-revolution of this pattern around the x axis.

The same pattern can also be obtained by locating source 1 at the origin of the coordinates and source 2 at a distance d along the positive x axis as indicated in Fig. 5−16*a*. Taking now the field from source 1 as reference, the field from source 2 in the direction ϕ is advanced by $d_r \cos\phi$. Thus, the total field E at a large distance r is the vector sum of the fields from the two sources as given by

$$E = E_0 + E_0 e^{+j\psi} \tag{5}$$

where $\psi = d_r \cos\phi$.

The relation of these fields is indicated by the vector diagram of Fig. 5−16*b*. From the vector diagram the magnitude of the total field is

$$E = 2E_0 \cos\frac{\psi}{2} = 2E_0 \cos\frac{d_r \cos\phi}{2} \tag{6}$$

as obtained before in (3). The phase of the total field E is, however, not constant in this case but is $\psi/2$, as also shown by rewriting (5) as

$$E = E_0(1 + e^{j\psi}) = 2E_0 e^{j\psi/2}\left(\frac{e^{j\psi/2} + e^{-j\psi/2}}{2}\right) = 2E_0 e^{j\psi/2}\cos\frac{\psi}{2} \tag{7}$$

Normalizing by setting $2E_0 = 1$, (7) becomes

$$E = e^{j\psi/2}\cos\frac{\psi}{2} = \cos\frac{\psi}{2}\angle\psi/2 \tag{8}$$

[1]It is to be noted that the quantities represented here by vectors are not true space vectors but merely vector representations of the time phase (i.e., phasors).

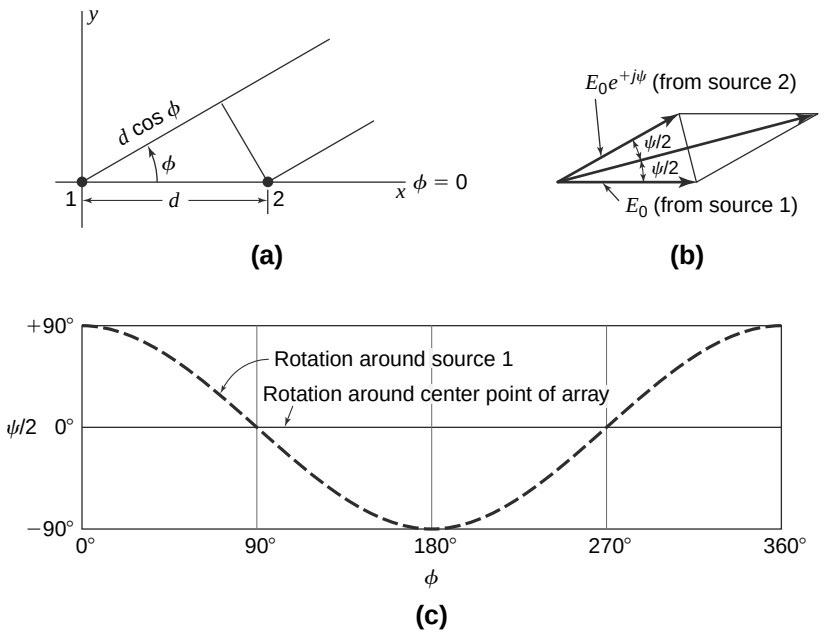

Figure 5–16 (*a*) Two isotropic point sources with the origin of the coordinate system coincident with one of the sources. (*b*) Vector addition of the fields from two isotropic point sources of equal amplitude and same phase located as in (*a*). (*c*) Phase of total field as a function of ϕ for two isotropic point sources of same amplitude and phase spaced $\lambda/2$ apart. The phase change is zero when referred to the center point of the array but is $\psi/2$ as shown by the dashed curve when referred to source 1.

In (8) the cosine factor gives the amplitude variation of E, and the exponential or angle factor gives the phase variation *with respect to source* 1 as the reference. The phase variation for the case of $\lambda/2$ spacing ($d_r = \pi$) is shown by the dashed line in Fig. 5−16*c*. Here the phase angle with respect to the phase of source 1 is given by $\psi/2 = (\pi/2)\cos\phi$. The magnitude variation for this case has already been presented in Fig. 5−15*c*. When the phase is referred to the point midway between the sources (Fig. 5−15*a*), there is no phase change around the array as shown by the solid line in Fig. 5−16*c*. Thus, an observer at a fixed distance observes no phase change when the array is rotated (with respect to ϕ) around its midpoint, but a phase change (dashed curve of Fig. 5−16*c*) is observed if the array is rotated with source 1 as the center of rotation.

Case 2. Two Isotropic Point Sources of Same Amplitude but Opposite Phase

This case is identical with the one we have just considered except that the two sources are in opposite phase instead of in the same phase. Let the sources be located as in Fig. 5−15*a*. Then the total field in the direction ϕ at a large distance r is given by

$$E = E_0 e^{+j\psi/2} - E_0 e^{-j\psi/2} \tag{9}$$

from which

$$E = 2jE_0 \sin\frac{\psi}{2} = 2jE_0 \sin\left(\frac{d_r}{2}\cos\phi\right) \tag{10}$$

whereas in Case 1 (3) involves the cosine of $\psi/2$, (10) for Case 2 involves the sine. Equation (10) also includes an operator j, indicating that the phase reversal of one of the sources in Case 2 results in a 90° phase shift of the total field as compared with the total field for Case 1. This is unimportant here. Thus, putting $2jE_0 = 1$ and considering the special case of $d = \lambda/2$, (10) becomes

$$E = \sin\left(\frac{\pi}{2}\cos\phi\right) \tag{11}$$

The directions ϕ_m of maximum field are obtained by setting the argument of (11) equal to $\pm(2k+1)\pi/2$. Thus,

$$\frac{\pi}{2}\cos\phi_m = \pm(2k+1)\frac{\pi}{2} \tag{11a}$$

where $k = 0, 1, 2, 3\ldots$. For $k = 0$, $\cos\phi_m = \pm 1$ and $\phi_m = 0°$ and 180°.

The null directions ϕ_0 are given by

$$\frac{\pi}{2}\cos\phi_0 = \pm k\pi \tag{11b}$$

For $k = 0$, $\phi_0 = \pm 90°$.

The half-power directions are given by

$$\frac{\pi}{2}\cos\phi = \pm(2k+1)\frac{\pi}{4} \tag{11c}$$

For $k = 0$, $\phi = \pm 60°, \pm 120°$.

The field pattern given by (11) is shown in Fig. 5−17. The pattern is a relatively broad figure-of-eight with the maximum field in the same direction as the line joining the sources (x axis). The space pattern is a figure-of-revolution of this pattern around the x axis. The two sources, in this case, may be described as a simple type of "end-fire" array. In contrast to this pattern, the in-phase point sources produce a pattern with the maximum field normal to the line joining the sources, as shown in Fig. 5−15*c*. The two sources for this case may be described as a simple "broadside" type of array.

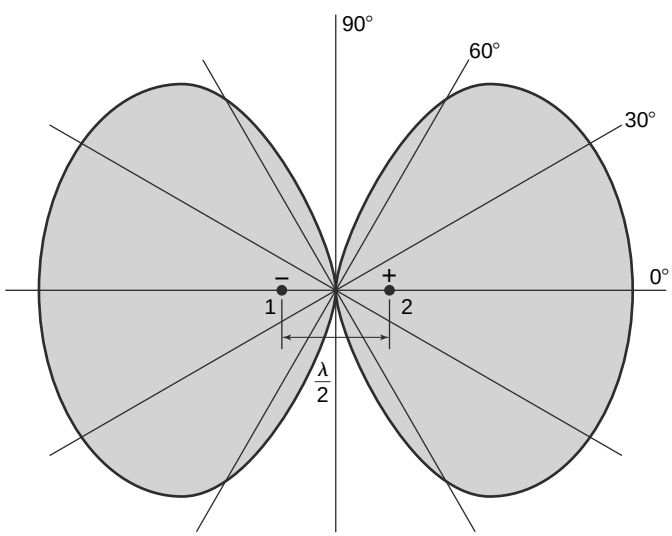

Figure 5–17 Relative field pattern for two isotropic point sources of the same amplitude but opposite phase, spaced $\lambda/2$ apart.

Case 3. Two Isotropic Point Sources of the Same Amplitude and In-Phase Quadrature

Let the two point sources be located as in Fig. 5−15*a*. Taking the origin of the coordinates as the reference for phase, let source 1 be retarded by 45° and source 2 advanced by 45°.

Then the total field in the direction ϕ at a large distance r is given by

$$E = E_0 \exp\left[+j\left(\frac{d_r \cos\phi}{2} + \frac{\pi}{4}\right)\right] + E_0 \exp\left[-j\left(\frac{d_r \cos\phi}{2} + \frac{\pi}{4}\right)\right] \tag{12}$$

From (12) we obtain

$$E = 2E_0 \cos\left(\frac{\pi}{4} + \frac{d_r}{2}\cos\phi\right) \tag{13}$$

Letting $2E_0 = 1$ and $d = \lambda/2$, (13) becomes

$$E = \cos\left(\frac{\pi}{4} + \frac{\pi}{2}\cos\phi\right) \tag{14}$$

The field pattern given by (14) is presented in Fig. 5−18. The space pattern is a figure-of-revolution of this pattern around the x axis. Most of the radiation is in the second and third quadrants. It is interesting to note that the field in the direction $\phi = 0°$ is the same as in the direction $\phi = 180°$. The directions ϕ_m of maximum field are obtained by setting the argument of (14) equal to $k\pi$, where $k = 0, 1, 2, 3 \ldots$. In this way we obtain

$$\frac{\pi}{4} + \frac{\pi}{2}\cos\phi_m = k\pi \tag{15}$$

For $k = 0$,

$$\frac{\pi}{2}\cos\phi_m = -\frac{\pi}{4} \tag{16}$$

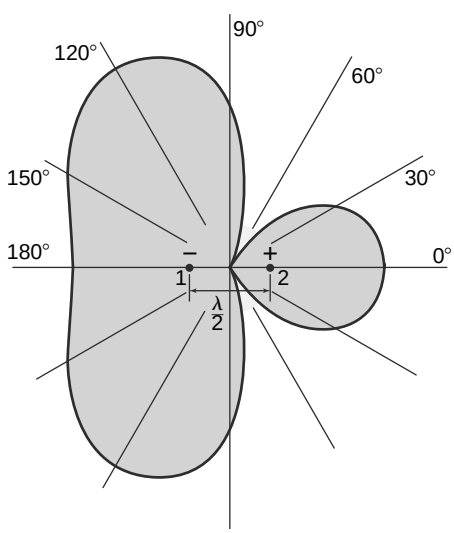

Figure 5–18 Relative field pattern of two isotropic point sources of the same amplitude and in phase quadrature for a spacing of $\lambda/2$. The source to the right leads that to the left by 90°.

and

$$\phi_m = 120^\circ \text{ and } 240^\circ \tag{17}$$

If the spacing between the sources is reduced to $\lambda/4$, (13) becomes

$$E = \cos\left(\frac{\pi}{4} + \frac{\pi}{4}\cos\phi\right) \tag{18}$$

The field pattern for this case is illustrated by Fig. 5−19*a*. It is a cardioid-shaped, unidirectional pattern with maximum field in the negative x direction. The space pattern is a figure-of-revolution of this pattern around the x axis.

A simple method of determining the direction of maximum field is illustrated by Fig. 5−19*b*. As indicated by the vectors, the phase of source 2 is 0° (vector to right) and the phase of source 1 is 270° (vector down). Thus, source 2 leads source 1 by 90°.

To find the field radiated to the left, imagine that we start at source 2 (phase 0°) and travel to the left, riding with the wave (phase 0°) like a surfer rides a breaker. The phase of the wave we are riding is 0° and does not change but by the time we have traveled $\lambda/4$ and arrived at source 1, a $\frac{1}{4}$-period has elapsed so the current in source 1 will have advanced 90° (vector rotated ccw) from 270° to 0°, making its phase the same as that of the wave we are riding, as in the middle diagram of Fig. 5−19*b*. Thus, the field of the wave from source 2 reinforces that of the field of source 1, and the two fields travel to the left together in phase producing a maximum field to the left which is twice the field of either source alone.

Now imagine that we start at source 1 with phase 270° (vector down) and travel to the right. By the time we arrive at source 2 the phase of its field has advanced from 0 to 90° so it is in phase opposition and cancels the field of the wave we are riding, as in the bottom diagram in Fig. 5−19*b*, resulting in zero radiation to the right.

Case 4. General Case of Two Isotropic Point Sources of Equal Amplitude and Any Phase Difference

Proceeding now to a more general situation, let us consider the case of two isotropic point sources of equal amplitude but of any phase difference δ. The total phase difference ψ between the fields from source 2 and source 1 at a distant point in the direction ϕ (see Fig. 5−16*a*) is then

$$\psi = d_r \cos\phi + \delta \tag{19}$$

Taking source 1 as the reference for phase, the positive sign in (19) indicates that source 2 is advanced in phase by the angle δ. A minus sign would be used to indicate a phase retardation. If, instead of referring the phase to source 1, it is referred to the centerpoint of the array, the phase of the field from source 1 at a distant point is given by $-\psi/2$ and that from source 2 by $+\psi/2$. The total field is then

$$E = E_0(e^{j\psi/2} + e^{-j\psi/2}) = 2E_0\cos\frac{\psi}{2} \tag{20}$$

Normalizing (20), we have the general expression for the field pattern of two isotropic sources of equal amplitude and arbitrary phase,

$$E = \cos\frac{\psi}{2} \tag{21}$$

where ψ is given by (19). The three cases we have discussed are obviously special cases of (21). Thus, Cases 1, 2, and 3 are obtained from (21) when $\delta = 0^\circ$, 180°, and 90° respectively.

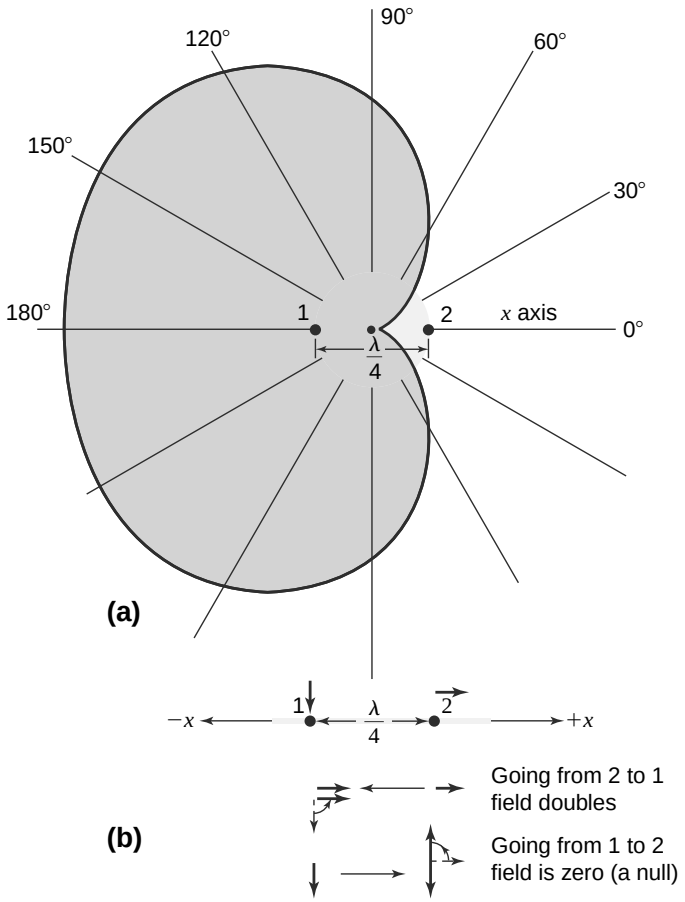

Figure 5–19 (*a*) Relative field pattern of two isotropic sources of same amplitude and in-phase quadrature for a spacing of $\lambda/4$. Source 2 leads source 1 by 90°. (*b*) Vector diagrams illustrating field reinforcement in the $-x$ direction and field cancellation in the $+x$ direction.

Case 5. Most General Case of Two Isotropic Point Sources of Unequal Amplitude and Any Phase Difference

A still more general situation, involving two isotropic point sources, exists when the amplitudes are unequal and the phase difference is arbitrary. Let the sources be situated as in Fig. 5−20*a* with source 1 at the origin. Assume that the source 1 has the larger amplitude and that its field at a large distance r has an amplitude of E_0. Let the field from source 2 be of amplitude aE_0 $(0 \le a \le 1)$ at the distance r. Then, referring to Fig. 5−20*b*, the magnitude and phase angle of the total field E is given by

$$E = E_0\sqrt{(1 + a\cos\psi)^2 + a^2\sin^2\psi}\ \angle[a\sin\psi/(1 + a\cos\psi)] \tag{22}$$

where $\psi = d_r\cos\phi + \delta$ and the phase angle ($\angle$) is referred to source 1. This is the phase angle ξ shown in Fig. 5−20*b*.

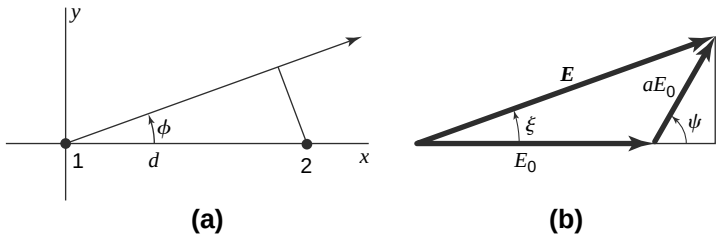

Figure 5–20 (*a*) Two isotropic point sources of unequal amplitude and arbitrary phase with respect to the coordinate system. (*b*) Vector addition of fields from unequal sources arranged as in (*a*). The amplitude of source 2 is assumed to be smaller than that of source 1 by the factor *a*.

5–10 Nonisotropic but Similar Point Sources and the Principle of Pattern Multiplication

The cases considered in the preceding section all involve *isotropic* point sources. These can readily be extended to a more general situation in which the sources are *nonisotropic but similar*.

The word *similar* is here used to indicate that the variation with absolute angle ϕ of both the amplitude and phase of the field is the same.[1] The maximum amplitudes of the individual sources may be unequal. If, however, they are also equal, the sources are not only similar but are *identical*.

As an example, let us reconsider Case 4 of Sec. 5−9 in which the sources are identical, with the modification that both sources 1 and 2 have field patterns given by

$$E_0 = E_0' \sin\phi \tag{1}$$

Patterns of this type might be produced by short dipoles oriented parallel to the x axis as suggested by Fig. 5−21. Substituting (1) in (5−9−20) and normalizing by setting $2E_0' = 1$ gives the field pattern of the array as

$$E = \sin\phi \cos\frac{\psi}{2} \tag{2}$$

where $\psi = d_r \cos\phi + \delta$

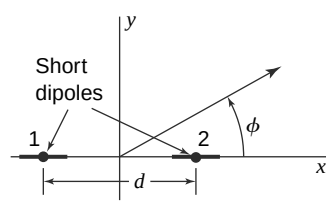

Figure 5–21 Two nonisotropic sources with respect to the coordinate system.

This result is the same as obtained by multiplying the pattern of the individual source ($\sin\phi$) by the pattern of two isotropic point sources ($\cos\psi/2$).

If the similar but unequal point sources of Case 5 (Sec. 5−9) have patterns as given by (1), the total normalized pattern is

$$E = \sin\phi\sqrt{(1 + a\cos\psi)^2 + a^2\sin^2\psi} \tag{3}$$

Here again, the result is the same as that obtained by multiplying the pattern of the individual source by the pattern of an array of isotropic point sources.

[1]The patterns not only must be of the same shape but also must be oriented in the same direction to be called "similar."

These are examples illustrating the ***principle of pattern multiplication,*** which may be expressed as follows:

> ***The field pattern of an array of nonisotropic but similar point sources is the product of the pattern of the individual source and the pattern of an array of isotropic point sources having the same locations, relative amplitudes, and phase as the nonisotropic point sources.***

This principle may be applied to arrays of any number of sources provided only that they are similar. The individual nonisotropic source or antenna may be of finite size but can be considered as a point source situated at the point in the antenna to which phase is referred. This point is said to be the "phase center."

The above discussion of pattern multiplication has been concerned only with the field pattern or magnitude of the field. If the field of the nonisotropic source and the array of isotropic sources vary in phase with space angle, i.e., have a phase pattern which is not a constant, the statement of the principle of pattern multiplication may be extended to include this more general case as follows:

> The total field pattern of an array of nonisotropic but similar sources is the product of the individual source pattern and the pattern of an array of isotropic point sources each located at the phase center of the individual source and having the same relative amplitude and phase, while the total phase pattern is the sum of the phase patterns of the individual source and the array of isotropic point sources.

The total phase pattern is referred to the phase center of the array. In symbols, the total field E is then

$$E = \underbrace{f(\theta,\phi)F(\theta,\phi)}_{\text{Field pattern}} \underbrace{/\, f_p(\theta,\phi) + F_p(\theta,\phi)}_{\text{Phase pattern}} \tag{4}$$

where

$f(\theta,\phi)$ = field pattern of individual source
$f_p(\theta,\phi)$ = phase pattern of individual source
$F(\theta,\phi)$ = field pattern of array of isotropic sources
$F_p(\theta,\phi)$ = phase pattern of array of isotropic sources

The patterns are expressed in (4) as a function of both polar angles to indicate that the principle of pattern multiplication applies to space patterns as well as to the two-dimensional cases we have been considering.

To illustrate the principle, let us apply to it two special modifications of Case 1 (Sec. 5−9).

EXAMPLE 5–10.1 Assume two identical point sources separated by a distance d, each source having the field pattern given by (1) as might be obtained by two short dipoles arranged as in Fig. 5−21. Let $d = \lambda/2$ and the phase angle $\delta = 0$. Then the total field pattern is

$$E = \sin\phi \cos\left(\frac{\pi}{2}\cos\phi\right) \tag{5}$$

This pattern is illustrated by Fig. 5−22*c* as the product of the individual source pattern ($\sin\phi$) shown at (*a*) and the array pattern $\{\cos[(\pi/2)\cos\phi]\}$ as shown at (*b*). The pattern is sharper than it was in Case 1 (Sec. 5−9) for the isotropic sources. In this instance, the maximum field of the individual source is in the direction $\phi = 90°$, which coincides with the direction of the maximum field for the array of two isotropic sources.

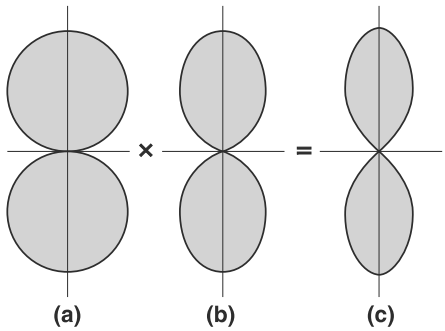

Figure 5–22 Example of pattern multiplication. Two nonisotropic but identical point sources of the same amplitude and phase, spaced $\lambda/2$ apart and arranged as in Fig. 5−21, produce the pattern shown at (*c*). The individual source has the pattern shown at (*a*), which, when multiplied by the pattern of an array of two isotropic point sources (of the same amplitude and phase) as shown at (*b*), yields the total array pattern of (*c*).

EXAMPLE 5–10.2 Let us consider next the situation in which $d = \lambda/2$ and $\delta = 0$ as in Example 5−10.1 but with individual source patterns given by

$$E_0 = E_0' \cos\phi \qquad (6)$$

This type of pattern might be produced by short dipoles oriented parallel to the y axis as in Fig. 5−23. Here the maximum field of the individual source is in the direction ($\phi = 0$) of a null from the array, while the individual source has a null in the direction ($\phi = 90°$) of the pattern maximum of the array. By the principle of pattern multiplication the total normalized field is

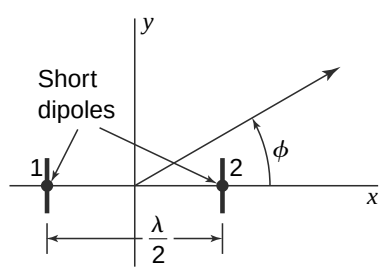

Figure 5–23 Array of two nonisotropic sources with respect to the coordinate system.

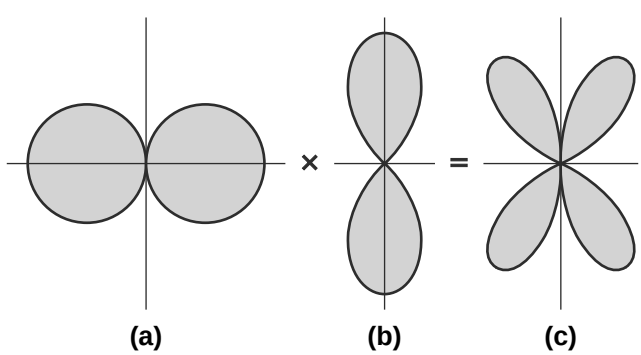

Figure 5–24 Example of pattern multiplication. Total array pattern (*c*) as the product of pattern (*a*) of individual nonisotropic source and pattern (*b*) of array of two isotropic sources. The pattern (*b*) for the array of two isotropic sources is identical with that of Fig. 5−22*b*, but the individual source pattern (*a*) is rotated through 90° with respect to the one in Fig. 5−22*a*.

$$E = \cos\phi \cos\left(\frac{\pi}{2}\cos\phi\right) \tag{7}$$

The total array pattern in the xy plane as given by (7) is illustrated in Fig. 5−24*c* as the product of the individual source pattern ($\cos\phi$) shown at (*a*) and the array pattern $\{\cos[(\pi/2)\cos\phi]\}$ shown at (*b*). The total array pattern in the xy plane has four lobes with nulls at the x and y axes.

The above examples illustrate two applications of the principle of pattern multiplication to arrays in which the source has a simple pattern. However, in the more general case the individual source may represent an antenna of any complexity provided that the amplitude and phase of its field can be expressed as a function of angle, that is to say, provided that the field pattern and the phase pattern with respect to the phase center are known. If only the total field pattern is desired, phase patterns need not be known provided that the individual sources are identical.

If the arrays in the above examples are parts of still larger arrays, the smaller arrays may be regarded as nonisotropic point sources in the larger array—another application of the principle of pattern multiplication yielding the complete pattern. In this way the principle of pattern multiplication can be applied n times to find the patterns of arrays of arrays of arrays.

5–11 Example of Pattern Synthesis by Pattern Multiplication

The principle of pattern multiplication, discussed in the preceding section, is of great value in pattern synthesis. By pattern synthesis is meant the process of finding the source or array of sources that produces a desired pattern. Theoretically an array of isotropic point sources can be found that will produce any arbitrary pattern. This process is not always simple and may yield an array that is difficult or impossible to construct. A simpler, less elegant approach to the problem of antenna synthesis is by the application of pattern multiplication to combinations of practical arrays, the combination which best approximates the desired pattern being arrived at by a trial-and-error process.

To illustrate this application of pattern multiplication, let us consider the following hypothetical problem. A broadcasting station (in the 500- to 1500-kHz frequency band) requires a pattern in the horizontal plane fulfilling the conditions indicated in Fig. 5−25*a*. The maximum field intensity, with as little variation as possible, is to be radiated in the 90° sector between northwest and northeast. No nulls in the pattern can occur in this sector. However, nulls may occur in any direction in the complementary 270° sector, but, as an additional requirement, nulls must be present in the due east and the due southwest directions in order to prevent interference with other stations in these directions. An idealized sector-shaped pattern fulfilling those requirements is illustrated in Fig. 5−25*b*. The antenna producing this pattern is to consist of an array of four vertical towers. The currents in all towers are to be equal in magnitude, but the phase

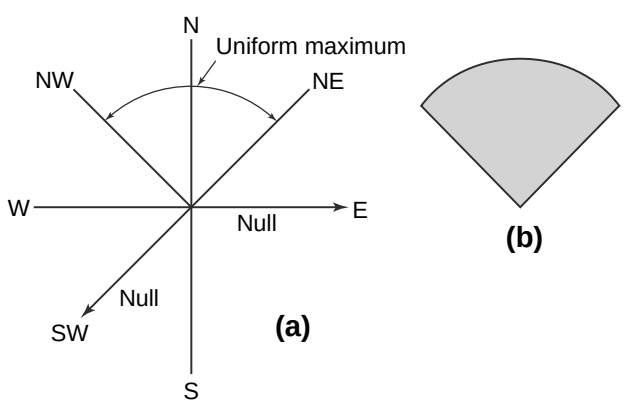

Figure 5–25 (*a*) Requirements for pattern of broadcast station and (*b*) idealized pattern fulfilling them.

may be adjusted to any relationship. There is also no restriction on the spacing or geometrical arrangement of the towers.

Since we are interested only in the horizontal plane pattern, each tower may be considered as an isotropic point source. The problem then becomes one of finding a space and phase relation of four isotropic point sources located in the horizontal plane which fulfills the above requirements.

The principle of pattern multiplication will be applied to the solution of this problem by seeking the patterns of two pairs of isotropic sources which yield the desired pattern when multiplied together. First let us find a pair of isotropic sources whose pattern fulfills the requirements of a broad lobe of radiation with maximum north and a null southwest. This will be called the "primary" pattern.

Two isotropic sources phased as an end-fire array can produce a pattern with a broader major lobe than when phased as a broadside array (for example, compare Figs. 5−15*c* and 5−19). Since a broad lobe to the north is desired, an end-fire arrangement of two isotropic sources as shown in Fig. 5−26 will be tried.

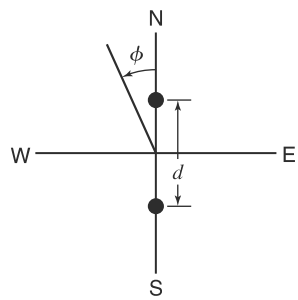

Figure 5–26 Arrangement of two isotropic point sources for both primary and secondary arrays.

From a consideration of pattern shapes as a function of separation and phase, a spacing between $\lambda/4$ and $3\lambda/8$ appears suitable (see Fig. 6−30). (See Brown-1, Terman-1, and Smith-1.) Accordingly, let $d = 0.3\lambda$. Then the field pattern for the array is

$$E = \cos\frac{\psi}{2} \tag{1}$$

where

$$\psi = 0.6\pi\cos\phi + \delta \tag{2}$$

For there to be a null in the pattern of (1) at $\phi = 135°$, it is necessary that[1]

$$\psi = (2k+1)\pi \tag{3}$$

where $k = 0, 1, 2, 3, \ldots$
Equating (2) and (3) then gives

$$-0.6\pi\frac{1}{\sqrt{2}} + \delta = (2k+1)\pi \tag{4}$$

or

$$\delta = (2k+1)\pi + 0.425\pi \tag{5}$$

For $k = 0$, $\delta = -104°$. The pattern for this case ($d = 0.3\lambda$ and $\delta = -104°$) is illustrated by Fig. 5−27*a*.

Next, let us find the array of two isotropic point sources that will produce a pattern that fulfills the requirements of a null at $\phi = 270°$ and that also has a broad lobe to the north. This will be called the "secondary" pattern. This pattern multiplied by the primary array pattern will then yield the total array

[1]The azimuth angle ϕ (Fig. 5−26) is measured counterclockwise (ccw) from the north. This is consistent with the engineering practice of measuring positive angles in a counterclockwise sense. However, it should be noted that the *geodetic azimuth angle* of a point is measured in the opposite, or clockwise (cw), sense from the reference direction, which is sometimes taken as south and sometimes as north.

pattern. If the secondary isotropic sources are also arranged as in Fig. 5−26 and have a phase difference of 180°, there is a null at $\phi = 270°$. Let the spacing $d = 0.6\lambda$. Then the secondary pattern is given by (1) where

$$\psi = 1.2\pi \cos\phi + \pi \tag{6}$$

The pattern is illustrated by Fig. 5−27*b*. By the principle of pattern multiplication, the total array pattern is the product of this pattern and the primary array pattern, or

$$E = \cos(54° \cos\phi - 52°) \cos(108° \cos\phi + 90°) \tag{7}$$

This pattern, which is illustrated by Fig. 5−27*c*, satisfies the pattern requirements. The complete array is obtained by replacing each of the isotropic sources of the secondary pattern by the two-source array producing the primary pattern. The midpoint of each primary array is its phase center, so this point is placed at the location of a secondary source. The complete antenna is then a linear array of four isotropic point sources as shown in the lower part of Fig. 5−27, where now each source represents a single vertical tower. All towers carry the same current. The current of tower 2 leads tower 1 and the current of tower 4 leads tower 3 by 104°, while the current in towers 1 and 3 and 2 and 4 are in phase opposition. The relative phase of the current is illustrated by the vectors in the lower part of Fig. 5−27*c*.

The solution obtained is only one of an infinite number of possible solutions involving four towers. It is, however, a satisfactory and practical solution to the problem.

The phase variation ξ around the primary, secondary, and total arrays is shown in Figs. 5−28*a*, *b*, and *c* with the phase center at the centerpoint of each array and also at the southernmost source. The arrangement of the arrays with their phase centers is illustrated in Fig. 5−28*d* for both cases.

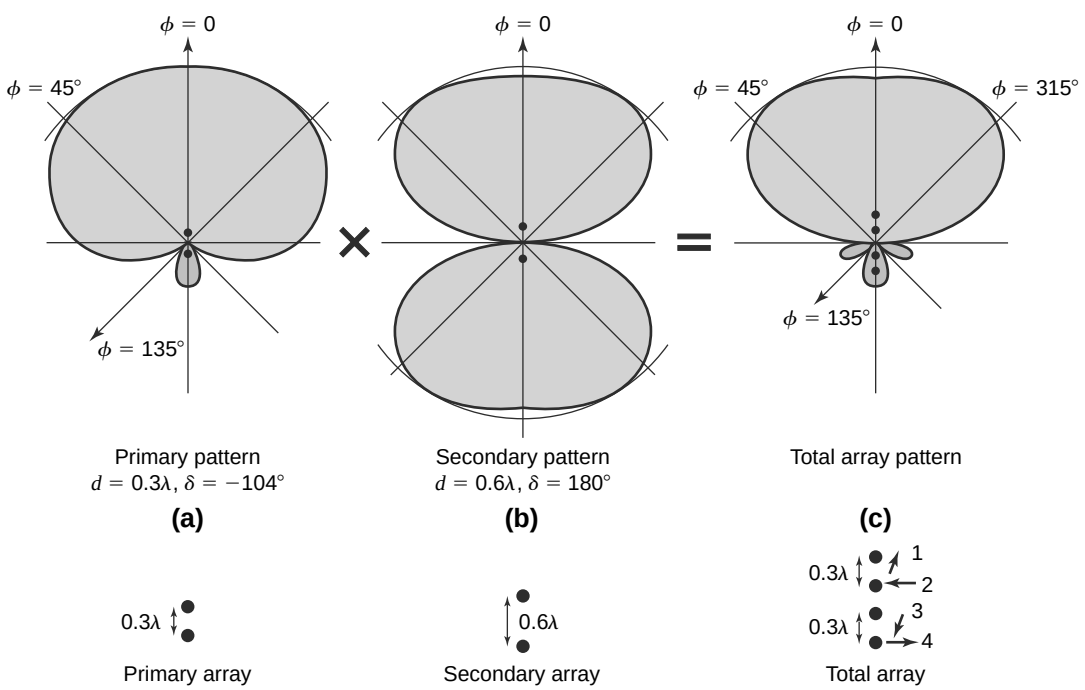

Figure 5–27 Field patterns of primary and secondary arrays of two isotropic sources which multiplied together give pattern of total array of four isotropic sources.

5–12 Nonisotropic and Dissimilar Point Sources

In Sec. 5−10 nonisotropic but similar point sources were discussed, and it was shown that the principle of pattern multiplication could be applied. However, if the sources are dissimilar, this principle is no longer applicable and the fields of the sources must be added at each angle ϕ for which the total field is calculated. Thus, for two dissimilar sources 1 and 2 situated on the x axis with source 1 at the origin and the sources separated by a distance d (same geometry as Fig. 5−20) the total field is in general

$$E = E_1 + E_2 = E_0\sqrt{[f(\phi) + aF(\phi)\cos\psi]^2 + [aF(\phi)\sin\psi]^2} \Big/ f_p(\phi) + \arctan[aF(\phi)\sin\psi/(f(\phi) + aF(\phi)\cos\psi)] \quad (1)$$

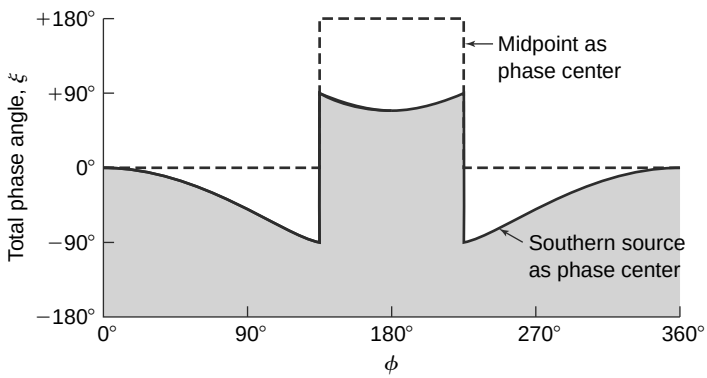

(a) Primary pattern

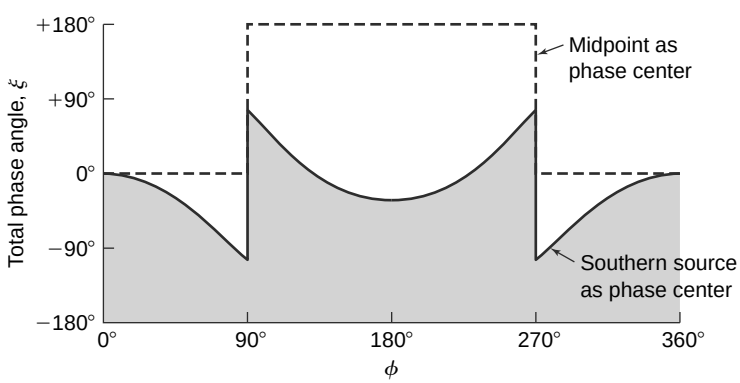

(b) Secondary pattern

Figure 5–28 Phase patterns of primary, secondary and total arrays having the field patterns shown in Fig. 5−27. Phase patterns are given for the phase center at the midpoint of the array and at the southernmost source, the arrangement of the arrays and the phase centers being shown at (*d*). The phase angle ξ is adjusted to zero at $\phi = 0$ in all cases.

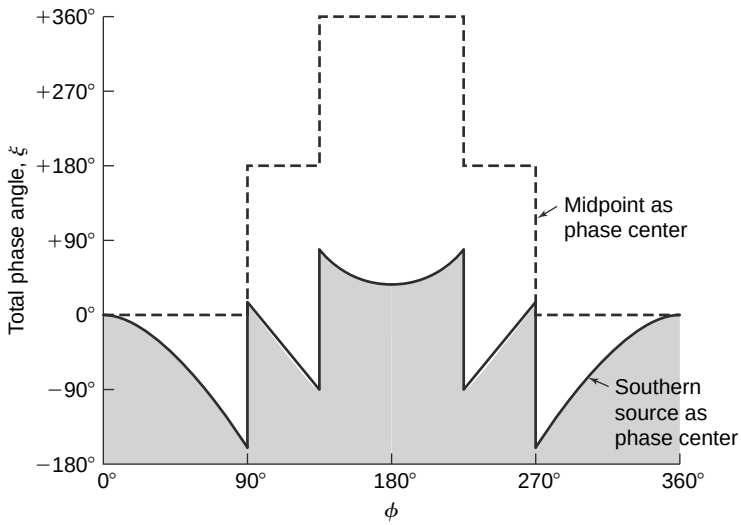

(c) Total pattern

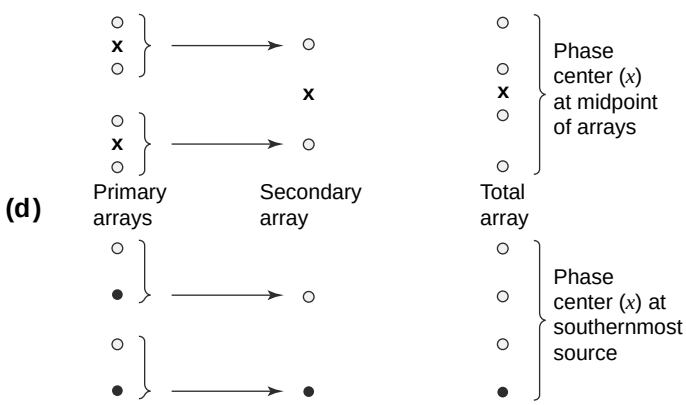

Figure 5–28 Continued.

where the field from source 1 is taken as

$$E_1 = E_0 f(\phi) \Big/ \underline{f_p(\phi)} \tag{2}$$

and from source 2 as

$$E_2 = aE_0 F(\phi) \Big/ \underline{F_p(\phi) + d_r \cos\phi + \delta} \tag{3}$$

where

E_0 = constant
a = ratio of maximum amplitude of source 2 to source 1 $(0 \le a \le 1)$
$\psi = d_r \cos\phi + \delta - f_p(\phi) + F_p(\phi)$, where
δ = relative phase of source 2 with respect to source 1

$f(\phi)$ = relative field pattern of source 1
$f_p(\phi)$ = phase pattern of source 1
$F(\phi)$ = relative field pattern of source 2
$F_p(\phi)$ = phase pattern of source 2

In (1) the phase angle ($\angle$) is referred to the phase of the field from source 1 in some reference direction ($\phi = \phi_0$).

In the special case where the field patterns are identical but the phase patterns are not, $a = 1$, and

$$f(\phi) = F(\phi) \tag{4}$$

from which

$$E = 2E_0 f(\phi) \cos\frac{\psi}{2} \angle f_p(\phi) + \psi/2 \tag{5}$$

where phase is again referred to source 1 in some reference direction ϕ_0.

As an illustration of nonisotropic, dissimilar point sources, let us consider an example in which the field from source 1 is given by

$$E_1 = \cos\phi \angle 0 \tag{6}$$

and from source 2 by

$$E_2 = \sin\phi \angle \psi \tag{7}$$

where $\psi = d_r \cos\phi + \delta$

The relation of the two sources to the coordinate system and the individual field patterns is shown in Fig. 5−29. Source 1 is located at the origin. The total field E is then the vector sum of E_1 and E_2, or

$$E = \cos\phi + \sin\phi \angle \psi \tag{8}$$

Let us consider the case for $\lambda/4$ spacing ($d = \lambda/4$) and phase quadrature of the sources ($\delta = \pi/2$). Then

$$\psi = \frac{\pi}{2}(\cos\phi + 1) \tag{9}$$

The calculation for this case is easily carried out by graphical vector addition. The resulting field pattern for the total field E of the array is presented in Fig. 5−30, and the resulting phase pattern for the angle ξ is given in Fig. 5–31. The angle ξ is the phase angle between the total field and the field of source 1 in the direction $\phi = 0$.

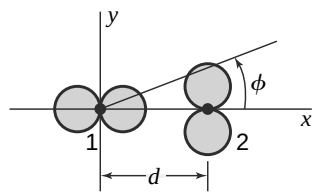

Figure 5–29 Relation of two nonisotropic dissimilar sources to coordinate system.

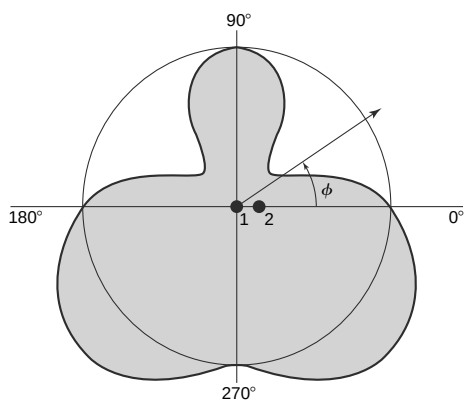

Figure 5–30 Field pattern of array of two nonisotropic dissimilar sources of Fig. 5−29 for $d = \lambda/4$ and $\delta = 90°$.

5–13 Linear Arrays of *n* Isotropic Point Sources of Equal Amplitude and Spacing

Introduction

Let us now proceed to the case of n isotropic point sources of equal amplitude and spacing arranged as a linear array, as indicated in Fig. 5−32, where n is any positive integer. The total field E at a large distance in the direction ϕ is given by

$$E = 1 + e^{j\psi} + e^{j2\psi} + e^{j3\psi} + \cdots + e^{j(n-1)\psi} \tag{1}$$

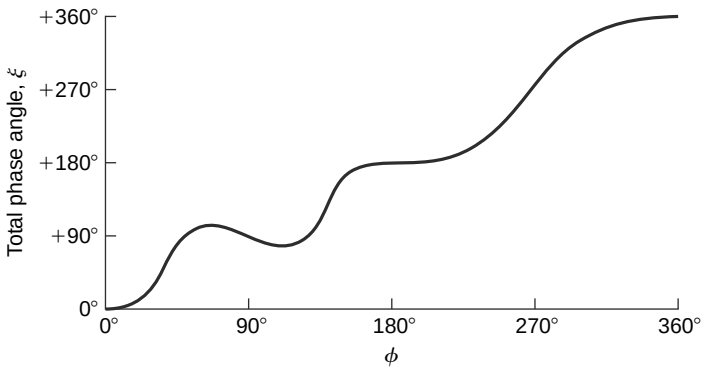

Figure 5–31 Phase pattern of array having field pattern of Fig. 5−30. The phase angle ξ is with respect to source 1 as phase center.

where ψ is the total phase difference of the fields from adjacent sources as given by

$$\psi = \frac{2\pi d}{\lambda}\cos\phi + \delta = d_r \cos\phi + \delta \qquad (2)$$

where δ is the phase difference of adjacent sources, i.e., source 2 with respect to 1, 3 with respect to 2, etc. (Schelkunoff-1, Stratton-1).

The amplitudes of the fields from the sources are all equal and taken as unity. Source 1 (Fig. 5−32) is the phase reference. Thus, at a distant point in the direction ϕ the field from source 2 is advanced in phase with respect to source 1 by ψ, the field from source 3 is advanced in phase with respect to source 1 by 2ψ, etc.

Equation (1) is a geometric series. Each term represents a phasor, and the amplitude of the total field E and its phase angle ξ can be obtained by phasor (vector) addition as in Fig. 5−33. Analytically, E can be expressed in a simple trigonometric form which we now develop as follows:

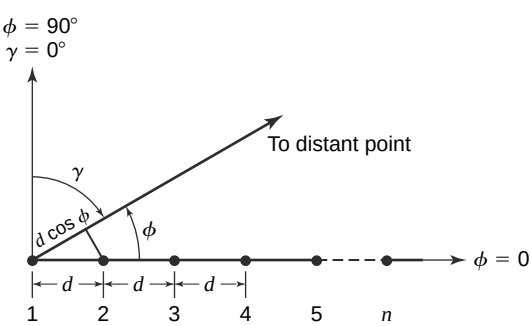

Figure 5–32 Arrangement of linear array of *n* isotropic point sources.

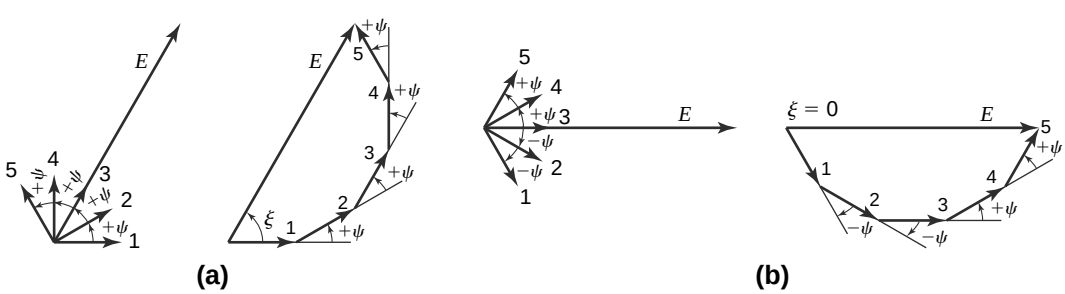

Figure 5–33 (*a*) Vector addition of fields at a large distance from the linear array of five isotropic point sources of equal amplitude with source 1 as the phase center (reference for phase). (*b*) Same, but with midpoint of array (source 3) as phase center.

Multiply (1) by $e^{j\psi}$, giving

$$Ee^{j\psi} = e^{j\psi} + e^{j2\psi} + e^{j3\psi} + \cdots + e^{jn\psi} \tag{3}$$

Now subtract (3) from (1) and divide by $1 - e^{j\psi}$, yielding

$$E = \frac{1 - e^{jn\psi}}{1 - e^{j\psi}} \tag{4}$$

Equation (4) may be rewritten as

$$E = \frac{e^{jn\psi/2}}{e^{j\psi/2}} \left(\frac{e^{jn\psi/2} - e^{-jn\psi/2}}{e^{j\psi/2} - e^{-j\psi/2}} \right) \tag{5}$$

from which

$$E = e^{j\xi} \frac{\sin(n\psi/2)}{\sin(\psi/2)} = \frac{\sin(n\psi/2)}{\sin(\psi/2)} \underline{/\xi} \tag{6}$$

where ξ is referred to the field from source 1. The value of ξ is given by

$$\xi = \frac{n-1}{2}\psi \tag{7}$$

If the phase is referred to the centerpoint of the array, (6) becomes

$$E = \frac{\sin(n\psi/2)}{\sin(\psi/2)} \tag{8}$$

In this case the phase pattern is a step function as given by the sign of (8). The phase of the field is constant wherever E has a value but changes sign when E goes through zero.

When $\psi = 0$, (6) or (8) is indeterminate so that for this case E must be obtained as the limit of (8) as ψ approaches zero. Thus, for $\psi = 0$ we have the relation that

$$E = n \tag{8a}$$

This is the maximum value that E can attain. Hence, the normalized value of the total field for $E_{\max} = n$ is

$$E = \frac{1}{n} \frac{\sin(n\psi/2)}{\sin(\psi/2)} \tag{9}$$

The field as given by (9) will be referred to as the "array factor." Values of the array factor as obtained from (9) for various numbers of sources are presented in Fig. 5−34. If ψ is known as a function of ϕ, then the field pattern can be obtained directly from Fig. 5−34.

We may conclude from the above discussion that the field from the array will be a maximum in any direction ϕ for which $\psi = 0$. Stated in another way, the fields from the sources all arrive at a distant point in the same phase when $\psi = 0$. In special cases, ψ may not be zero for any value of ϕ, and in this case the field is usually a maximum at the minimum value of ψ.

To illustrate some of the properties of linear arrays (9) will now be applied to several special cases. See programs on the book's web site involving these different cases. See also discussion in Appendix C.

Case 1. Broadside Array (Sources in Phase)

The first case is a linear array of n isotropic sources of the same amplitude and phase. Therefore, $\delta = 0$ and

$$\psi = d_r \cos\phi \tag{10}$$

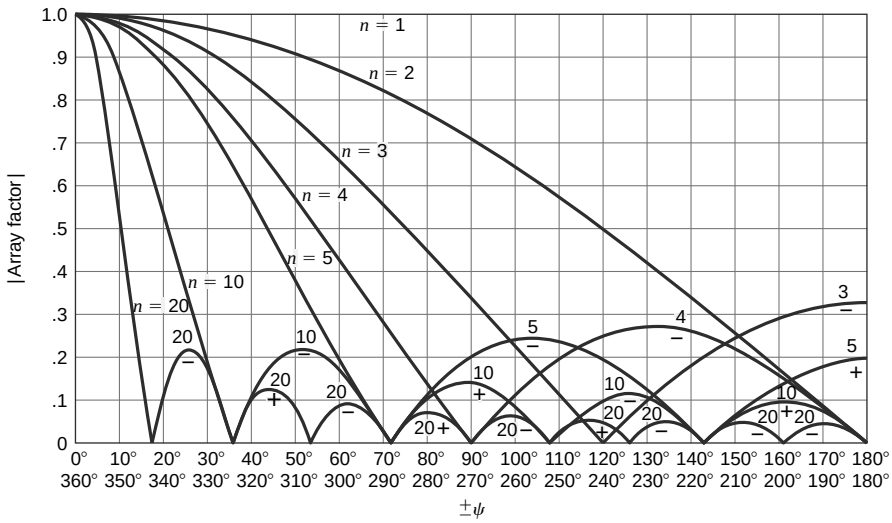

Figure 5–34 Universal field-pattern chart for arrays of various numbers *n* of isotropic point sources of equal amplitude and spacing.

To make $\psi = 0$ requires that $\phi = (2k+1)(\pi/2)$, where $k = 0, 1, 2, 3, \ldots$. The field is, therefore, a maximum when

$$\phi = \frac{\pi}{2} \qquad \text{and} \qquad \frac{3\pi}{2} \tag{10a}$$

That is, the maximum field is in a direction normal to the array. Hence, this condition, which is characterized by in-phase sources ($\delta = 0$), results in a "broadside" type of array.

As an example, the pattern of a broadside array of four in-phase isotropic point sources of equal amplitude is shown in Fig. 5−35*a*. The spacing between sources is $\lambda/2$.[1] The field pattern in rectangular coordinates and the phase patterns for this array are presented in Fig. 5−35*a*.

Case 2. Ordinary End-Fire Array

Let us now find the phase angle between adjacent sources that is required to make the field a maximum in the direction of the array ($\phi = 0$). An array of this type may be called an "end-fire" array. For this we substitute the conditions $\psi = 0$ and $\phi = 0$ into (2), from which

$$\delta = -d_r \tag{11}$$

Hence, for an end-fire array, the phase between sources is retarded progressively by the same amount as the spacing between sources in radians. Thus, if the spacing is $\lambda/4$, source 2 in Fig. 5−32 should lag source 1 by 90°, source 3 should lag source 2 by 90°, etc.

As an example, the field pattern of an end-fire array of four isotropic point sources is presented in Fig. 5−36*a*. The spacing between sources is $\lambda/2$ and $\delta = -\pi$. The field pattern in rectangular coordinates and the phase patterns are shown in Fig. 5−36*b*. The same shape of field pattern is obtained in this case if $\delta = +\pi$ since, with $d = \lambda/2$, the pattern is bidirectional. However, if the spacing is less than $\lambda/2$, the maximum radiation is in the direction $\phi = 0$ when $\delta = -d_r$ and in the direction $\phi = 180°$ when $\delta = +d_r$.

[1] If the spacing between elements exceeds λ, sidelobes appear which are equal in amplitude to the main (center) lobe. These are called *grating lobes* (see Sec. 19−6)

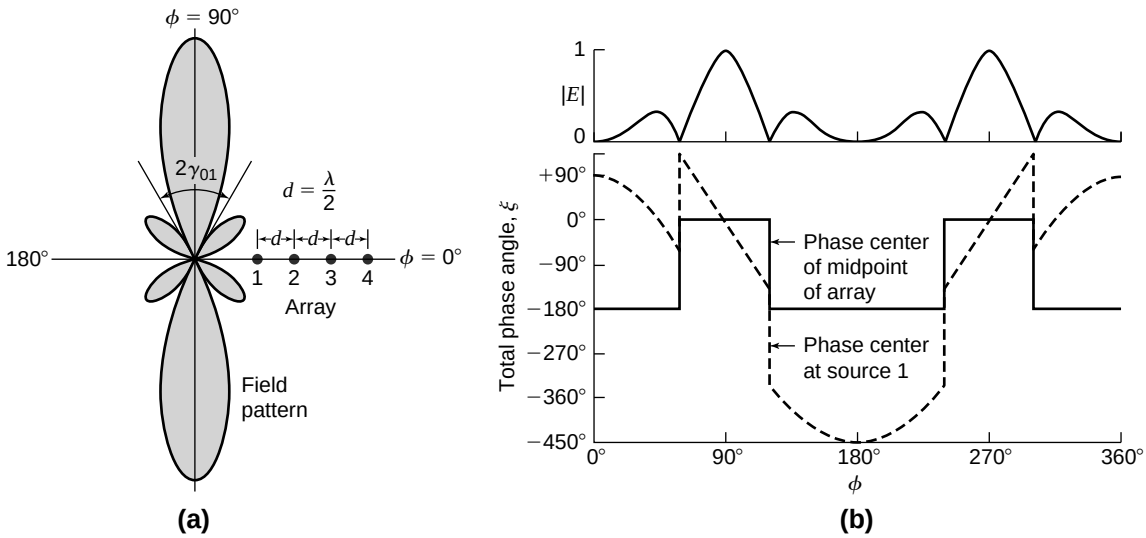

Figure 5–35 (*a*) Field pattern of broadside array of four isotropic point sources of the same amplitude and phase. The spacing between sources is $\lambda/2$. (*b*) Field pattern in rectangular coordinates and phase patterns of same array with phase center at midpoint and at source 1. The reference direction for phase is at $\phi = 90°$.

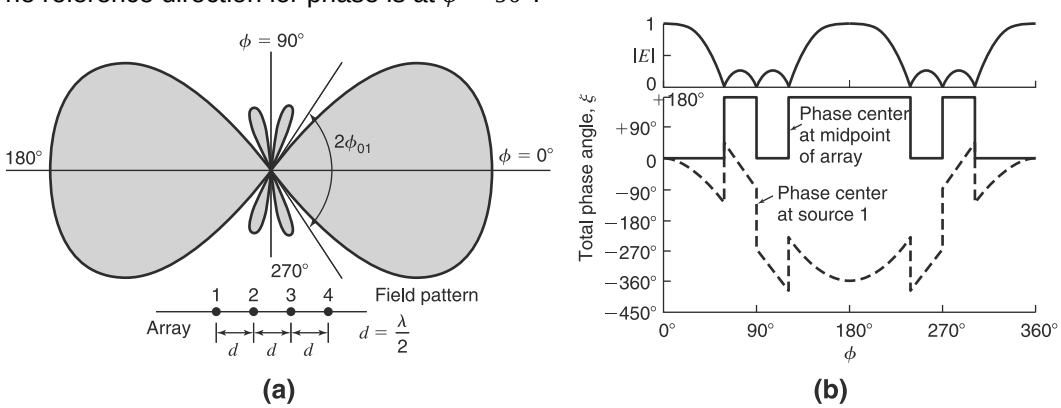

Figure 5–36 (*a*) Field pattern of ordinary end-fire array of four isotropic point sources of same amplitude. Spacing is $\lambda/2$ and the phase angle $\delta = -\pi$. (*b*) Field pattern in rectangular coordinates and phase patterns of same array with phase center at midpoint and at source 1. The reference direction for phase is at $\phi = 0$.

Case 3. End-Fire Array with Increased Directivity

The situation discussed in Case 2, namely, for $\delta = -d_r$, produces a maximum field in the direction $\phi = 0$ but does not give the maximum directivity. It has been shown by Hansen (1) and Woodyard that a larger directivity is obtained by increasing the phase change between sources so that

$$\delta = -\left(d_r + \frac{\pi}{n}\right) \tag{12}$$

This condition will be referred to as the condition for "increased directivity." Thus for the phase difference of the fields at a large distance we have

$$\psi = d_r(\cos\phi - 1) - \frac{\pi}{n} \tag{13}$$

As an example, the field pattern of an end-fire array of four isotropic point sources for this case is illustrated in Fig. 5–37.

The spacing between sources is $\lambda/2$, and therefore $\delta = -(5\pi/4)$. Hence, the conditions are the same as for the array with the pattern of Fig. 5–36, except that the phase difference between sources is increased by $\pi/4$. Comparing the field patterns of Figs. 5–36*a* and 5–37, it is apparent that the additional phase difference yields a considerably sharper main lobe in the direction $\phi = 0$. However, the back lobes in this case are excessively large because the large value of spacing results in too great a range in ψ.

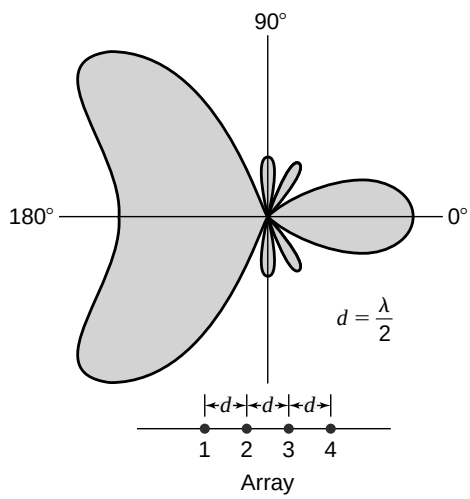

Figure 5–37 Field pattern of end-fire array of four isotropic point sources of equal amplitude spaced $\lambda/2$ apart. The phasing is adjusted for increased directivity ($\delta = -\frac{5}{4}\pi$).

To realize the directivity increase afforded by the additional phase difference requires that $|\psi|$ be restricted in its range to a value of π/n at $\phi = 0$ and a value in the vicinity of π at $\phi = 180°$. This can be fulfilled if the spacing is reduced. For example, the field pattern of an end-fire array of 10 isotropic point sources of equal amplitude and spaced $\lambda/4$ apart is presented in Fig. 5–38*a* for the phase condition giving increased directivity ($\delta = -0.6\pi$). In contrast to this pattern, one is presented in Fig. 5–38*b* for the identical antenna with the phasing of an ordinary end-fire array ($\delta = -0.5\pi$). Both patterns are plotted to the same maximum. The increased directivity is apparent from the greater sharpness of the pattern. Integrating the pattern, including the minor lobes, the directivity is found to be about 19 and of the ordinary endfire about 11. The beamwidths and directivities for the two cases are compared in Table 5–2.

Table 5–2 Comparison of end-fire arrays

	Ordinary end-fire array	End-fire array with increased directivity
Beamwidth between half-power points	69°	38°
Beamwidth between first nulls	106°	74°
Directivity	11	19

The maximum of the field pattern of Fig. 5–38*a* occurs at $\phi = 0$ and $\psi = -\pi/n$. In general, any increased directivity end-fire array, with maximum at $\psi = -\pi/n$, has a normalized field pattern given by

$$E = \sin\left(\frac{\pi}{2n}\right)\frac{\sin(n\psi/2)}{\sin(\psi/2)} \tag{14}$$

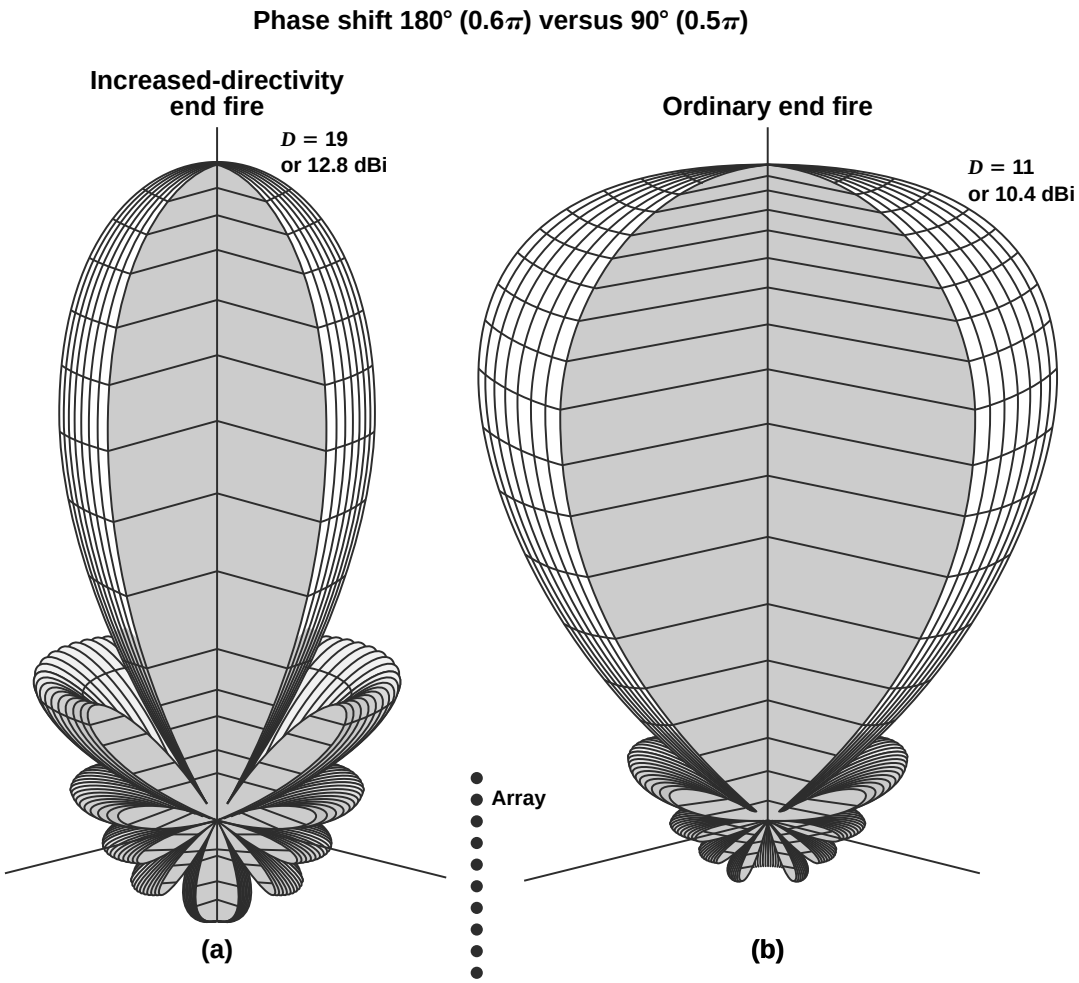

Figure 5–38 Field patterns of end-fire arrays of 10 isotropic point sources of equal amplitude spaced $\lambda/4$ apart. The pattern at (*a*) has the phase adjusted for increased directivity ($\delta = -0.6\pi$), while the pattern at (*b*) has the phasing of an ordinary end-fire array ($\delta = -0.5\pi$).

Case 4. Array with Maximum Field in an Arbitrary Direction. Scanning Array

Let us consider the case of an array with a field pattern having a maximum in some arbitrary direction ϕ_1 not equal to $k\pi/2$ where $k = 0, 1, 2,$ or 3. Then (2) becomes

$$0 = d_r \cos\phi_1 + \delta \tag{15}$$

By specifying the spacing d_r, the required phase difference δ is then determined by (15). Conversely, by changing δ the beam direction ϕ_1 can be shifted or scanned.

As an example, suppose that $n = 4$, $d = \lambda/2$, and that we wish to have a maximum field in the direction of $\phi = 60°$. Then $\delta = -\pi/2$, yielding the field pattern shown in Fig. 5−39.

5–14 Null Directions for Arrays of *n* Isotropic Point Sources of Equal Amplitude and Spacing

In this section simple methods are discussed for finding the directions of the pattern nulls of the arrays considered in Sec. 5−13.

Following the procedure given by Schelkunoff (2, 3) the null directions for an array of n isotropic point sources of equal amplitude and spacing occur when $E = 0$ or, provided that the denominator of Eq. (5−13−4) is not zero, when

$$e^{jn\psi} = 1 \tag{1}$$

Equation (1) requires that

$$n\psi = \pm 2K\pi \tag{2}$$

where $K = 1, 2, 3, \ldots$

Equating the value of ψ in (2) to its value in Eq. (5−13−2) gives

$$\psi = d_r \cos\phi_0 + \delta = \pm\frac{2K\pi}{n} \tag{3}$$

Thus,

$$\phi_0 = \arccos\left[\left(\pm\frac{2K\pi}{n} - \delta\right)\frac{1}{d_r}\right] \tag{4}$$

where ϕ_0 gives the direction of the pattern nulls. Note that values of K must be excluded for which $K = mn$, where $m = 1, 2, 3, \ldots$. Thus, if $K = mn$, (2) reduces to $\psi = \pm 2m\pi$ and the denominator of Eq. (5−13−4) equals zero so that the null condition of (1), that the numerator of Eq. (5−13−4) be zero, is insufficient.

In a broadside array $\delta = 0$, so that for this case (4) becomes

$$\phi_0 = \arccos\left(\pm\frac{2K\pi}{nd_r}\right) = \arccos\left(\pm\frac{K\lambda}{nd}\right) \tag{5}$$

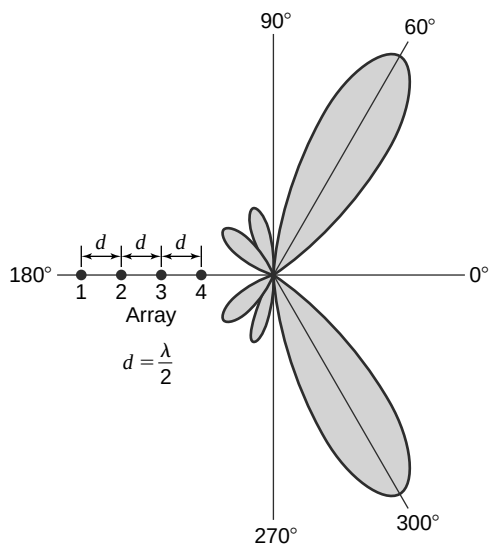

Figure 5–39 Field pattern of array of four isotropic point sources of equal amplitude with phasing adjusted to give the maximum at $\phi = 60°$. The spacing is $\lambda/2$.

As an example, the field pattern of Fig. 5−35 ($n = 4$, $d = \lambda/2$, $\delta = 0$) has the null directions

$$\phi_0 = \arccos\left(\pm\frac{K}{2}\right) \tag{6}$$

For $K = 1$, $\phi_0 = \pm 60°$ and $\pm 120°$, and for $K = 2$, $\phi_0 = 0°$ and $180°$. These are the six null directions for this array.

If ϕ_0 in (3) is replaced by its complementary angle γ_0 (see Fig. 5−32), then (5) becomes

$$\gamma_0 = \arcsin\left(\pm\frac{K\lambda}{nd}\right) \tag{7}$$

If the array is long, so that $nd \gg K\lambda$,

$$\gamma_0 \simeq \pm\frac{K\lambda}{nd} \tag{8}$$

The first nulls either side of the maximum occur for $K = 1$. These angles will be designated γ_{01}. Thus,

$$\gamma_{01} \simeq \pm\frac{\lambda}{nd} \tag{9}$$

and the total beamwidth of the main lobe between first nulls *for a long broadside array* is then

$$2\gamma_{01} \simeq \frac{2\lambda}{nd} \tag{10}$$

For the field pattern in Fig. 5−35 this width is exactly 60°, while as given by (10) it is 1 rad, or 57.3°. This pattern is for an array 2λ long. The agreement would be better with longer arrays.

Turning next to *end-fire arrays*, the condition for an ordinary end-fire array is that $\delta = -d_r$. Thus, for this case (3) becomes

$$\cos\phi_0 - 1 = \pm\frac{2K\pi}{nd_r} \tag{11}$$

from which we obtain

$$\frac{\phi_0}{2} = \arcsin\left(\pm\sqrt{\frac{K\pi}{nd_r}}\right) \tag{12}$$

or

$$\phi_0 = 2\arcsin\left(\pm\sqrt{\frac{K\lambda}{2nd}}\right) \tag{13}$$

As an example, the field pattern of Fig. 5−36 ($n = 4, d = \lambda/2, \delta = -\pi$) has the null directions

$$\phi_0 = 2\arcsin\left(\pm\sqrt{\frac{K}{4}}\right) \tag{14}$$

For $K = 1, \phi_0 = \pm 60°$; for $K = 2, \phi_0 = \pm 90°$, etc.
If the array is long, so that $nd \gg K\lambda$, (13) becomes

$$\phi_0 \simeq \pm\sqrt{\frac{2K\lambda}{nd}} \tag{15}$$

The first nulls either side of the main lobe occur for $K = 1$. These angles will be designated ϕ_{01}. Thus,

$$\phi_{01} \simeq \pm\sqrt{\frac{2\lambda}{nd}} \tag{16}$$

and the total beamwidth of the main lobe between first nulls *for a long ordinary end-fire array* is then

$$2\phi_{01} \simeq 2\sqrt{\frac{2\lambda}{nd}} \tag{17}$$

For the field pattern in Fig. 5−36 this width is exactly 120°, while as given by (17) it is 2 rad, or 115°.

For end-fire arrays with increased directivity as proposed by Hansen (1) and Woodyard, the condition is that $\delta = -(d_r + \pi/n)$. Thus, for this case (3) becomes

$$d_r(\cos\phi_0 - 1) - \frac{\pi}{n} = \pm 2\frac{K\pi}{n} \tag{18}$$

from which

$$\frac{\phi_0}{2} = \arcsin\left[\pm\sqrt{\frac{\pi}{2nd_r}(2K-1)}\right] \tag{19}$$

or

$$\phi_0 = 2\arcsin\left[\pm\sqrt{\frac{\lambda}{4nd}(2K-1)}\right] \tag{20}$$

If the array is long, so that $nd \gg K\lambda$, (20) becomes

$$\phi_0 \simeq \pm\sqrt{\frac{\lambda}{nd}(2K-1)} \tag{21}$$

The first nulls either side of the main lobe, ϕ_{01}, occur for $K = 1$. Thus,

$$\phi_{01} \simeq \pm\sqrt{\frac{\lambda}{nd}} \tag{22}$$

and the total beamwidth of the main lobe between first nulls *for a long end-fire array with increased directivity* is then

$$2\phi_{01} \simeq 2\sqrt{\frac{\lambda}{nd}} \tag{23}$$

This width is $1/\sqrt{2}$, or 71 percent, of the width of the ordinary end-fire array. As an example, the ordinary end-fire array pattern of Fig. 5−38*b* has a beamwidth between first nulls of 106°. The width of the pattern in Fig. 5−38*a* for the array with increased directivity is 74°, or 70 percent as much.

Table 4.3 lists the formulas for null directions and beamwidths for the different arrays considered above. The null directions in column 2 apply to arrays of any length. The formulas in the third and fourth columns are approximate and apply only to long arrays.

The formulas in Table 5−3 have been used to calculate the curves presented in Fig. 5−40. These curves show the beamwidth between first nulls as a function of nd_λ for three types of arrays: broadside, ordinary end-fire, and end-fire with increased directivity. The quantity $nd_\lambda (= nd/\lambda)$ is approximately equal to the length of the array in wavelengths for long arrays. The exact value of the array length is $(n-1)d_\lambda$.

The beamwidth of long broadside arrays is inversely proportional to the array length, whereas the beamwidth of long end-fire types is inversely proportional to the square root of the array length. Hence,

Table 5–3 Null directions and beamwidths between first nulls for linear arrays of *n* isotropic point sources of equal amplitude and spacing. (For $n \geq 2$. The angles in columns 3 and 4 are expressed in radians. To convert to degrees, multiply by 57.3)

Type of array	Null directions (array any length)	Null directions (long array)	Beamwidth between first nulls (long array)
General case	$\phi_0 = \arccos\left[\left(\frac{\pm 2K\pi}{n} - \delta\right)\frac{1}{d_r}\right]$		
Broadside	$\gamma_0 = \arcsin\left(\pm\frac{K\lambda}{nd}\right)$	$\gamma_0 \simeq \pm\frac{K\lambda}{nd}$	$2\gamma_{01} \simeq \frac{2\lambda}{nd}$
Ordinary end-fire	$\phi_0 = 2\arcsin\left(\pm\sqrt{\frac{K\lambda}{2nd}}\right)$	$\phi_0 \simeq \pm\sqrt{\frac{2K\lambda}{nd}}$	$2\phi_{01} \simeq 2\sqrt{\frac{2\lambda}{nd}}$
End-fire with increased directivity (Hansen and Woodyard)	$\phi_0 = 2\arcsin\left[\pm\sqrt{\frac{\lambda}{4nd}(2K-1)}\right]$	$\phi_0 \simeq \pm\sqrt{\frac{\lambda}{nd}(2K-1)}$	$2\phi_{01} \simeq 2\sqrt{\frac{\lambda}{nd}}$

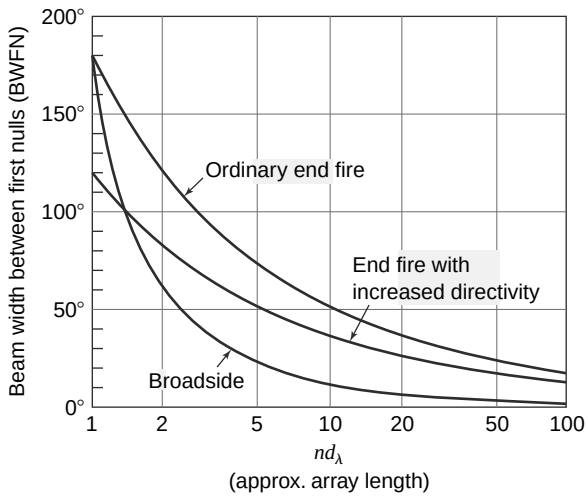

Figure 5–40 Beamwidth between first nulls as a function of nd_λ for arrays of n isotropic point sources of equal amplitude. For long arrays, nd_λ is approximately equal to the array length.

the beamwidth in the plane of a long linear broadside array is much smaller than for end-fire types of the same length as shown by Fig. 5−40. It should be noted, however, that the broadside array has a disk-shaped pattern with a narrow beamwidth in a plane through the array axis but a circular pattern (360° beamwidth) in the plane normal to the array axis. On the other hand, the end-fire array has a cigar-shaped pattern with the same beamwidth in all planes through the array axis.

5–15 Linear Broadside Arrays with Nonuniform Amplitude Distributions. General Considerations

Let us begin by comparing the field patterns of four amplitude distributions, namely, *uniform*, *binomial*, *edge*, and *optimum*. To be specific, we will consider a linear array of five isotropic point sources with $\lambda/2$ spacing. If the sources are in phase and all equal in amplitude, we may calculate the pattern as discussed in Sec. 5−13 the result being as shown in Fig. 5−41 by the pattern designated *uniform*. *A uniform distribution yields the maximum directivity* or gain. The pattern has a half-power beamwidth of 23°, but the side lobes are relatively large. The amplitude of the first side lobe is 24 percent of the main-lobe maximum. In some applications this minor-lobe amplitude may be undesirably large.

Table 5–4

n	Relative amplitudes (Pascal's triangle)									
3			1		2		1			
4		1		3		3		1		
5	1		4		6		4		1	
6	1	5		10		10		5		1

To reduce the Side-Lobe Level (SLL) of linear in-phase broadside arrays, John Stone Stone (1) proposed that the sources have amplitudes proportional to the coefficients of a binomial series of the form

$$(a+b)^{n-1} = a^{n-1} + (n-1)a^{n-2}b + \frac{(n-1)(n-2)}{2!}a^{(n-3)}b^2 + \cdots \tag{1}$$

where n is the number of sources. Thus, for arrays of three to six sources the relative amplitudes are given by Table 5−4, where the amplitudes are arranged as in *Pascal's triangle* (any inside number is equal to the sum of the adjacent numbers in the row above).

Applying the binomial distribution to the array of five sources spaced $\lambda/2$ apart, the sources have the relative amplitudes 1, 4, 6, 4, 1. The resulting pattern, designated *binomial*, is shown in Fig. 5−41. Methods of calculating such patterns are discussed in the next section. The pattern has no minor lobes, but this has been achieved at the expense of an increased beamwidth (31°). For spacings of $\lambda/2$ or less between elements, the minor lobes are eliminated by Stone's binomial distribution. However, the increased beamwidth and the large ratio of current amplitudes required in large arrays are disadvantages.

At the other extreme from the binomial distribution, we might try an edge distribution in which only the end sources of the array are supplied with power, the three central sources being either omitted or inactive. The relative amplitudes of the five-source array are, accordingly, 1, 0, 0, 0, 1. The array has, therefore, degenerated to two sources 2λ apart and has the field pattern designated as *edge* in Fig. 5−41. The beamwidth between half-power points of the "main" lobe (normal to the array) is 15°, but "minor" lobes are the same amplitude as the "main" lobe.

Table 5–5

Type of distribution	Half-power beamwidth	Minor-lobe amplitude (% of major lobe)
Binomial	31°	0
Edge	15°	100

Comparing the binomial and edge distributions for the five-source array with $\lambda/2$ spacing, we have Table 5−5.

Although for most applications it would be desirable to combine the 15° beamwidth of the edge distribution with the zero side-lobe level of the binomial distribution, this combination is not possible. However, if the distribution is between the binomial and the edge type, a compromise between the beamwidth and the side-lobe level can be made; i.e., the side-lobe level will not be zero, but the beamwidth will be less than for the binomial distribution. An amplitude distribution of this nature for linear in-phase broadside arrays was proposed by Dolph (1) which has the further property of ***optimizing*** the relation between beamwidth and side-lobe level; i.e., ***if the side-lobe level is specified, the beamwidth between first nulls is minimized;*** or, conversely, ***if the beamwidth between first nulls is specified, the side-lobe level is minimized.*** Dolph's distribution is based on the properties of the Tchebyscheff polynomials and accordingly will be referred to as the Dolph-Tchebyscheff or optimum distribution.

Applying the Dolph-Tchebyscheff distribution to our array of five sources with $\lambda/2$ spacing, let us specify a side-lobe level 20 dB below the main lobe, i.e., a minor-lobe amplitude 10 percent of the main lobe. The relative amplitude distribution for this side-lobe level is 1, 1.6, 1.9, 1.6, 1 and yields the pattern designated *optimum* in Fig. 5−41. Methods of calculating the distribution and pattern are discussed in the next section. The beamwidth between half-power points is 27°, which is less than for the binomial distribution. Smaller beamwidths can be obtained only by raising the side-lobe level. The Dolph-Tchebyscheff distribution includes all distributions between the binomial and the edge. In fact, the binomial and edge distributions are special cases of the Dolph-Tchebyscheff distribution, the binomial distribution corresponding to an infinite ratio between main- and side-lobe levels and the edge distribution to a ratio of unity. The uniform distribution is, however, not a special case of the Dolph-Tchebyscheff distribution.

Referring to Fig. 5−41, we may draw a number of general conclusions regarding the relation between patterns and amplitude distributions. We note that if the amplitude tapers to a small value at the edge of the

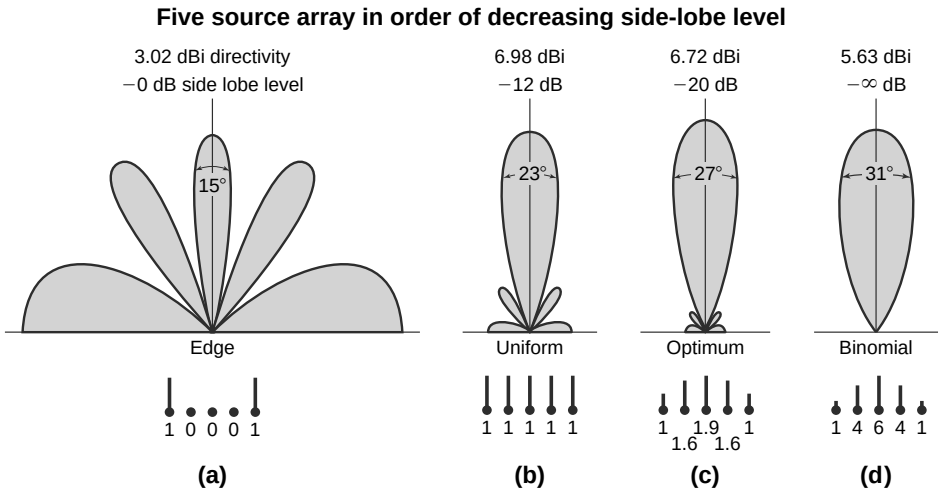

Figure 5–41 Normalized field patterns of broadside arrays of five isotropic point sources spaced $\lambda/2$ apart. All sources are in the same phase, but the relative amplitudes have four different distributions: edge, uniform, optimum, and binomial. Only the upper half of the pattern is shown. The relative amplitudes of the five sources are indicated in each case by the array below the pattern, the height of the line at each source being proportional to its amplitude. All patterns are adjusted to the same maximum amplitude.

array (binomial distribution), minor lobes can be eliminated. On the other hand, if the distribution has an inverse taper with maximum amplitude at the edges and none at the center of the array (edge distribution), the minor lobes are accentuated, being in fact equal to the "main" lobe. From this we may quite properly conclude that the side-lobe level is closely related to the abruptness with which the amplitude distribution ends at the edge of the array. An abrupt discontinuity in the distribution results in large minor lobes, while a gradually tapered distribution approaching zero at the edge minimizes the discontinuity and the minor-lobe amplitude. In the next section, we shall see that the abrupt discontinuity produces large higher "harmonic" terms in the Fourier series representing the pattern. On the other hand, these higher harmonic terms are small when the distribution tapers gradually to a small value at the edge. There is an analogy between this situation and the Fourier analysis of wave shapes. Thus, a square wave has relatively large higher harmonics, whereas a pure sine wave has none, the square wave being analogous to the uniform array distribution while the pure sine wave is analogous to the binomial distribution.

The preceding discussion has been concerned with arrays of discrete sources separated by finite distances. However, the general conclusions concerning amplitude distributions which we have drawn can be extended to large arrays of continuous distributions of an infinite number of point sources, such as might exist in the case of a continuous current distribution on a metal sheet or in the case of a continuous field distribution across the mouth of an electromagnetic horn or across a parabolic reflector antenna. If the amplitude distribution follows a Gaussian error curve, which is similar to a binomial distribution for discrete sources, then minor lobes are absent but the beamwidth is relatively large. An increase of amplitude at the edge reduces the beamwidth but results in minor lobes, as we have seen. Thus, in the case of a high-gain parabolic reflector type of antenna, the illumination of the reflector by the primary antenna is usually arranged to taper toward the edge of the parabola. However, a compromise is generally made between beamwidth and side-lobe level so that the illumination is not zero at the edge but has an appreciable value as in a Dolph-Tchebyscheff distribution.

Chapter 6

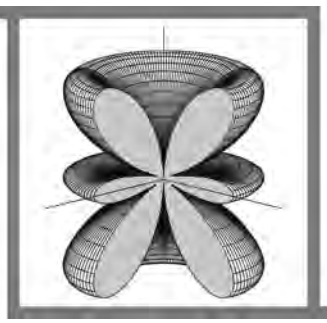

Electric Dipoles, Thin Linear Antennas and Arrays of Dipoles and Apertures

Topics in this chapter include:

- Fields of Short dipole
- Radiation resistance of Short dipole
- Thin linear antenna: $\lambda/2$, λ, and $3\lambda/2$
- Radiation resistance of $\lambda/2$ dipole
- Arrays of two $\lambda/2$ dipoles
- Broadside, end-fire and close-spaced arrays
- Radiation resistance at a point which is not a current maximum
- Traveling wave antennas
- Arrays of two driven elements; broadside and end-fire
- Patterns, driving point impedance and gain
- Arrays of two driven elements; general case
- Closely spaced elements
- Radiation efficiency
- Arrays of n driven elements
- Horizontal and vertical antennas above ground
- Shaped dipole arrays
- Phased arrays
- Grid and chain arrays
- Digital beam-forming or adaptive or smart arrays
- Long-wire antennas: V, Rhombic and Beverage
- Curtain arrays
- Arrays feed points
- Folded dipoles

6–1 Introduction

This chapter first develops the concepts of electric dipoles and thin linear antennas. Later it is extended to the arrays of dipoles and apertures. The essential background for this later part is covered in chap. 5 on point sources and their arrays. The dipoles referred to herein are mostly thin linear dipoles, whereas the apertures in general may be helices, horns, big reflectors or arrays of dipoles (arrays of arrays).

The far or radiation field pattern, the driving point impedance and the array gains are first derived in that order for several different arrays of dipoles. The method of analysis is general and applicable to other dipole arrays; the specific types discussed are merely examples. Array gain is calculated by treating the dipoles as circuit elements having self and mutual impedances. Although direct pattern integration could be used to determine the gain, the circuit approach is simpler provided impedance values are available (patterns having been utilized in the impedence calculations).

6–2 The Short Electric Dipole

Since any linear antenna may be considered as consisting of a large number of very short conductors connected in series, it is of interest to examine first the radiation properties of short conductors. From a knowledge of properties of short conductors, we can then proceed to a study of long linear conductors such as are commonly employed in practice.

A short linear conductor is often called a *short dipole*. In the following discussion, a short dipole is always of finite length even though it may be very short. If the dipole is vanishingly short, it is an infinitesimal dipole.

Let us consider a short dipole such as shown in Fig. 6–1*a*. The length L is very short compared to the wavelength ($L \ll \lambda$). Plates at the ends of the dipole provide capacitive loading. The short length and the presence of these plates result in a uniform current I along the entire length L of the dipole. The dipole may be energized by a balanced transmission line, as shown. It is assumed that the transmission line does not radiate and, therefore, its presence will be disregarded. Radiation from the end plates is also considered to be negligible. The diameter d of the dipole is small compared to its length ($d \ll L$). Thus, for purposes of analysis we may consider that the short dipole appears as in Fig. 6–1*b*. Here it consists simply of a thin conductor of length L with a uniform current I and point charges q at the ends. The current and charge are related by

$$\frac{dq}{dt} = I \tag{1}$$

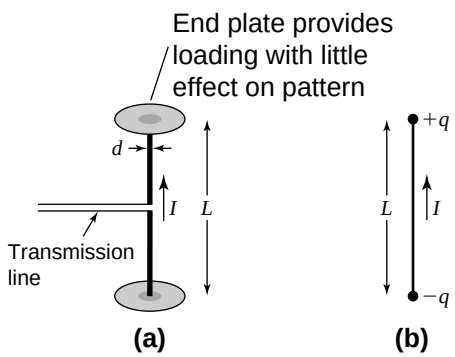

Figure 6–1 A short dipole antenna (*a*) and its equivalent (*b*).

6–3 The Fields of a Short Dipole

Let us now proceed to find the fields everywhere around a short dipole. Let the dipole of length L be placed coincident with the z axis and with its center at the origin as in Fig. 6–2. The relation of the electric field components, E_r, E_θ and E_ϕ, is then as shown. It is assumed that the medium surrounding the dipole is air or vacuum.

In dealing with antennas or radiating systems, the propagation time is a matter of great importance. Thus, if a current is flowing in the short dipole of Fig. 6–3, the effect of the current is not felt instantaneously at the point P, but only after an interval equal to the time required for the disturbance to propagate over the distance r. We have already recognized this in Chap. 5 in connection with the pattern of arrays of point sources, but here we are more explicit and describe it as a *retardation* effect.

Accordingly, instead of writing the current I as[1]

$$I = I_0 e^{j\omega t} \tag{1}$$

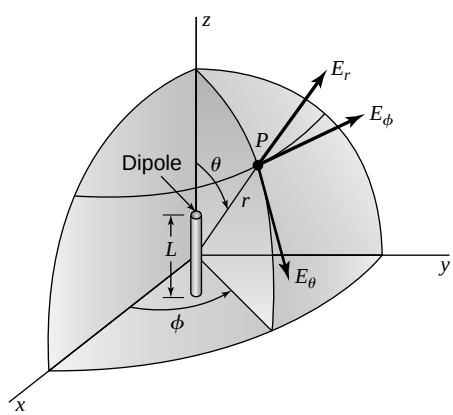

Figure 6–2 Relation of dipole to coordinates.

[1]It is assumed that we take either the real ($\cos \omega t$) or imaginary ($\sin \omega t$) part of $e^{j\omega t}$.

which implies instantaneous propagation of the effect of the current, we introduce the propagation (or retardation) time as done by Lorentz and write

$$[I] = I_0 e^{j\omega[t-(r/c)]} \tag{2}$$

where $[I]$ is called the *retarded current*. Specifically, the retardation time r/c results in a *phase retardation* $\omega r/c = 2\pi f r/c$ radians $= 360° \, fr/c = 360° \, t/T$, where $T = 1/f =$ time of one period or cycle (seconds) and $f =$ frequency (hertz, Hz = cycles per second). The brackets may be added as in (2) to indicate explicitly that the effect of the current is retarded.

Equation (2) is a statement of the fact that the disturbance at a time t and at a distance r from a current element is caused by a current $[I]$ that occurred at an earlier time $t - r/c$. The time difference r/c is the interval required for the disturbance to travel the distance r, where c is the velocity of light ($= 300$ Mm s^{-1}).

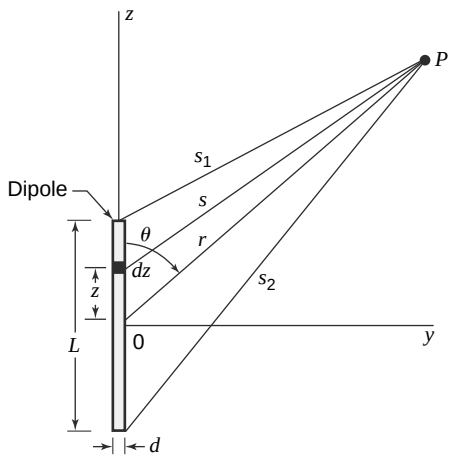

Figure 6–3a Geometry for short dipole.

Electric and magnetic fields can be expressed in terms of vector and scalar potentials. Since we will be interested not only in the fields near the dipole but also at distances which are large compared to the wavelength, we must use *retarded potentials*, i.e., expressions involving $t - r/c$. For a dipole located as in Fig. 6–2 or Fig. 6–3*a*, the retarded vector potential of the electric current has only one component, namely, A_z. Its value is

$$A_z = \frac{\mu_0}{4\pi} \int_{-L/2}^{L/2} \frac{[I]}{s} \, dz \tag{2}$$

where $[I]$ is the retarded current given by

$$[I] = I_0 e^{j\omega[t-(s/c)]} \tag{3a}$$

In (3) and (3a),

$z =$ distance to a point on the conductor
$I_0 =$ peak value in time of current (uniform along dipole)
$\mu_0 =$ permeability of free space $= 4\pi \times 10^{-7}$ H m^{-1}

If the distance from the dipole is large compared to its length ($r \gg L$) and if the wavelength is large compared to the length ($\lambda \gg L$), we can put $s = r$ and neglect the phase differences of the field contributions from different parts of the wire. The integrand in (3) can then be regarded as a constant, so that (3) becomes

$$A_z = \frac{\mu_0 L I_0 e^{j\omega[t-(r/c)]}}{4\pi r} \tag{4}$$

The retarded scalar potential V of a charge distribution is

$$V = \frac{1}{4\pi\varepsilon_0} \int_V \frac{[\rho]}{s} \, d\tau \tag{5}$$

where $[\rho]$ is the retarded charge density given by

$$[\rho] = \rho_0 e^{j\omega[t-(s/c)]} \tag{6}$$

and $d\tau$ = infinitesimal volume element

ε_0 = permittivity or dielectric constant of free space = 8.85×10^{-12} F m^{-1}

Since the region of charge in the case of the dipole being considered is confined to the points at the ends as in Fig. 6–1*b*, (5) reduces to

$$V = \frac{1}{4\pi\varepsilon_0}\left\{\frac{[q]}{s_1} - \frac{[q]}{s_2}\right\} \tag{7}$$

From (6–1–1) and (3a),

$$[q] = \int [I]\,dt = I_0 \int e^{j\omega[t-(s/c)]}\,dt = \frac{[I]}{j\omega} \tag{8}$$

Substituting (8) into (7),

$$V = \frac{I_0}{4\pi\varepsilon_0 j\omega}\left[\frac{e^{j\omega[t-(s_1/c)]}}{s_1} - \frac{e^{j\omega[t-(s_2/c)]}}{s_2}\right] \tag{9}$$

Referring to Fig. 6–3*b*, when $r \gg L$, the lines connecting the ends of the dipole and the point P may be considered as parallel so that

$$s_1 = r - \frac{L}{2}\cos\theta \tag{10}$$

and

$$s_2 = r + \frac{L}{2}\cos\theta \tag{11}$$

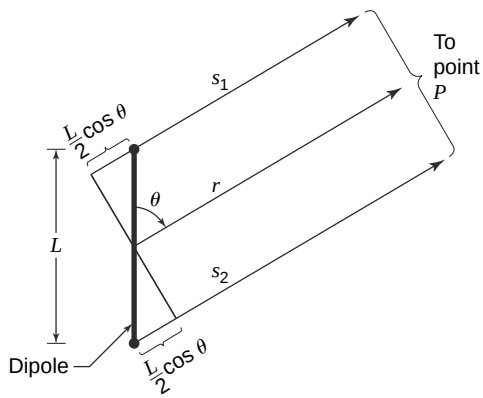

Figure 6–3b Relations for short dipole when $r \gg L$.

Substituting (10) and (11) into (9), it may be shown that the fields of a short electric dipole are:

Electric fields of short dipole — ***General case***

$$E_r = \frac{I_0 L\cos\theta e^{j\omega[t-(r/c)]}}{2\pi\varepsilon_0}\left(\frac{1}{cr^2} + \frac{1}{j\omega r^3}\right) \tag{12}$$

$$E_\theta = \frac{I_0 L\sin\theta e^{j\omega[t-(r/c)]}}{4\pi\varepsilon_0}\left(\frac{j\omega}{c^2 r} + \frac{1}{cr^2} + \frac{1}{j\omega r^3}\right) \tag{13}$$

In obtaining (12) and (13) the relation was used that $\mu_0\varepsilon_0 = 1/c^2$, where c = velocity of light. Turning our attention now to the ***magnetic field,*** this may be calculated from curl of A as follows:

$$\nabla \times \mathbf{A} = \frac{\hat{\mathbf{r}}}{r\sin\theta}\left[\frac{\partial(\sin\theta)A_\phi}{\partial\theta} - \frac{\partial(A_\theta)}{\partial\phi}\right] + \frac{\hat{\theta}}{r\sin\theta}\left[\frac{\partial A_r}{\partial\phi} - \frac{\partial(r\sin\theta)A_\phi}{\partial r}\right] + \frac{\hat{\phi}}{r}\left[\frac{\partial(rA_\theta)}{\partial r} - \frac{\partial A_r}{\partial\theta}\right] \tag{14}$$

Since $A_\phi = 0$, the first and fourth terms of (14) are zero, since A_r and A_θ are independent of ϕ, so that the second and third terms of (14) are also zero. Thus, only the last two terms contribute, so that $\nabla \times \mathbf{A}$, and hence also $\mathbf{H}$, have only a ϕ component. Thus,

Magnetic fields of short dipole

$$|\mathbf{H}| = H_\phi = \frac{I_0 L \sin\theta e^{j\omega[t-(r/c)]}}{4\pi}\left(\frac{j\omega}{cr} + \frac{1}{r^2}\right) \quad \textit{General case} \tag{15}$$

$$H_r = H_\theta = 0 \tag{16}$$

Thus, the fields from the dipole have only three components E_r, E_θ and H_ϕ. The components E_ϕ, H_r and H_θ are everywhere zero.

When r is very large, the terms in $1/r^2$ and $1/r^3$ in (12), (13), and (15) can be neglected in favor of the terms in $1/r$. Thus, in the *far field* E_r is negligible, and we have effectively only two field components, E_θ and H_ϕ, given by

Electric and magnetic fields of short dipole

$$E_\theta = \frac{j\omega I_0 L \sin\theta e^{j\omega[t-(r/c)]}}{4\pi\varepsilon_0 c^2 r} = j\frac{I_0\beta L}{4\pi\varepsilon_0 cr}\sin\theta e^{j\omega[t-(r/c)]} \tag{17}$$

$$H_\phi = \frac{j\omega I_0 L \sin\theta e^{j\omega[t-(r/c)]}}{4\pi cr} = j\frac{I_0\beta L}{4\pi r}\sin\theta e^{j\omega[t-(r/c)]} \quad \textit{Far-field case} \tag{18}$$

Taking the ratio of E_θ to H_ϕ as given by (17) and (18), we obtain

$$\frac{E_\theta}{H_\phi} = \frac{1}{\varepsilon_0 c} = \sqrt{\frac{\mu_0}{\varepsilon_0}} = 376.7\ \Omega \quad \textit{Impedance of space} \tag{19}$$

This is the ***intrinsic impedance of free space*** (a pure resistance). It is a very important constant.

Comparing (17) and (18) we note that E_θ and H_ϕ are in time phase in the far field. We note also that the field patterns of both are proportional to $\sin\theta$. The pattern is independent of ϕ, so that the space pattern is doughnut-shaped, being a figure-of-revolution of the pattern in Fig. 6–4*a* about the axis of the dipole. Referring to the near-field expressions given by (12), (13) and (15), we note that for a small r the electric field has two components E_r and E_θ, which are both in time-phase quadrature with the magnetic field, as in a resonator. At intermediate distances, E_θ and E_r can approach time-phase quadrature so that the total electric field vector rotates in a plane parallel to the direction of propagation, thus exhibiting the phenomenon of *cross-field*. For the E_θ and H_ϕ components, the near-field patterns are the same as the far-field patterns, being proportional to $\sin\theta$ (Fig. 6–4*a*). However, the near-field pattern for E_r is proportional to $\cos\theta$ as indicated by Fig. 6–4*b*. The space pattern for E_r is a figure-of-revolution of this pattern around the dipole axis.

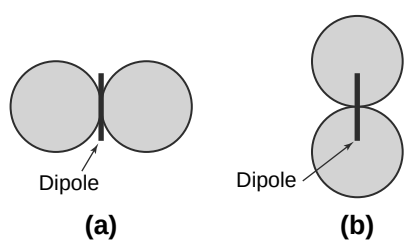

Figure 6–4 Near- and far-field patterns of E_θ and H_ϕ components for short dipole (*a*) and near-field pattern of E_r component (*b*).

Let us now consider the situation at very low frequencies. This will be referred to as the *quasi-stationary*, or dc case. Since from

$$[I] = I_0 e^{j\omega[t-(r/c)]} = j\omega[q] \tag{20}$$

(12) and (13) can be rewritten as

$$E_r = \frac{[q]L\cos\theta}{2\pi\varepsilon_0}\left(\frac{j\omega}{cr^2}+\frac{1}{r^3}\right) \tag{21}$$

and

$$E_\theta = \frac{[q]L\sin\theta}{4\pi\varepsilon_0}\left(-\frac{\omega^2}{c^2r}+\frac{j\omega}{cr^2}+\frac{1}{r^3}\right) \tag{22}$$

The magnetic field is given by (15) as

$$H_\phi = \frac{[I]L\sin\theta}{4\pi}\left(\frac{j\omega}{cr}+\frac{1}{r^2}\right) \tag{23}$$

At low frequencies, ω approaches zero so that the terms with ω in the numerator can be neglected. As $\omega \to 0$, we also have

$$[q] = q_0 e^{j\omega[t-(r/c)]} = q_0 \tag{24}$$

and

$$[I] = I_0 \tag{25}$$

Thus, for the quasi-stationary, or dc, case, the field components become from (21), (22) and (23)

Electric and magnetic fields of short dipole ***Low-frequency case***

$$E_r = \frac{q_0 L\cos\theta}{2\pi\varepsilon_0 r^3} \tag{26}$$

$$E_\theta = \frac{q_0 L\sin\theta}{4\pi\varepsilon_0 r^3} \tag{27}$$

$$H_\phi = \frac{I_0 L\sin\theta}{4\pi r^2} \tag{28}$$

The restriction that $r \gg L$ still applies.

The expressions for the electric field, (26) and (27), are identical to those obtained in electrostatics for the field of two point charges, $+q_0$ and $-q_0$, separated by a distance L. The relation for the magnetic field, (28), may be recognized as the Biot-Savart relation for the magnetic field of a short element carrying a steady or slowly varying current. Since in the expressions for the quasi-stationary case the fields decrease as $1/r^2$ or $1/r^3$, the fields are confined to the vicinity of the dipole and there is negligible radiation. In the general expressions for the fields, (21), (22) and (23), it is the $1/r$ terms which are important in the far field and hence take into account the radiation.

The expressions for the fields from a short dipole developed above are summarized in Table 6–1.

Setting

$$|A| = \frac{1}{2r_\lambda}$$

$$|B| = \frac{1}{4\pi r_\lambda^2}$$

$$|C| = \frac{1}{8\pi^2 r_\lambda^3}$$

Table 6–1 Fields of a short electric dipole†

Component	General expression	Far field	Quasi-stationary
E_r	$\frac{[I]L\cos\theta}{2\pi\varepsilon_0}\left(\frac{1}{cr^2}+\frac{1}{j\omega r^3}\right)$	0	$\frac{q_0 L\cos\theta}{2\pi\varepsilon_0 r^3}$
E_θ	$\frac{[I]L\sin\theta}{4\pi\varepsilon_0}\left(\frac{j\omega}{c^2 r}+\frac{1}{cr^2}+\frac{1}{j\omega r^3}\right)$	$\frac{[I]Lj\omega\sin\theta}{4\pi\varepsilon_0 c^2 r}=\frac{j60\pi[I]\sin\theta}{r}\frac{L}{\lambda}$	$\frac{q_0 L\sin\theta}{4\pi\varepsilon_0 r^3}$
H_ϕ	$\frac{[I]L\sin\theta}{4\pi}\left(\frac{j\omega}{cr}+\frac{1}{r^2}\right)$	$\frac{[I]Lj\omega\sin\theta}{4\pi cr}=\frac{j[I]\sin\theta}{2r}\frac{L}{\lambda}$	$\frac{I_0 L\sin\theta}{4\pi r^2}$

†The restriction applies that $r \gg L$ and $\lambda \gg L$. The quantities in the table are in SI units, that is, E in volts per meter, H in amperes per meter, I in amperes, r in meters, etc. $[I]$ is as given by (20). Three of the field components of an electric dipole are everywhere zero, that is,

$$E_\phi = H_r = H_\theta = 0$$

for the three components of E_θ, their variation with distance is as shown in Fig. 6–5. For r_λ greater than the radian distance $[1/(2\pi)]$, component A of the electric field is dominant, for r_λ less than the radian distance component C of the electric field is dominant, while *at* the radian distance only B contributes $(=\pi)$ because although $|A| = |B| = |C| = \pi$, A and C are in phase opposition and cancel.

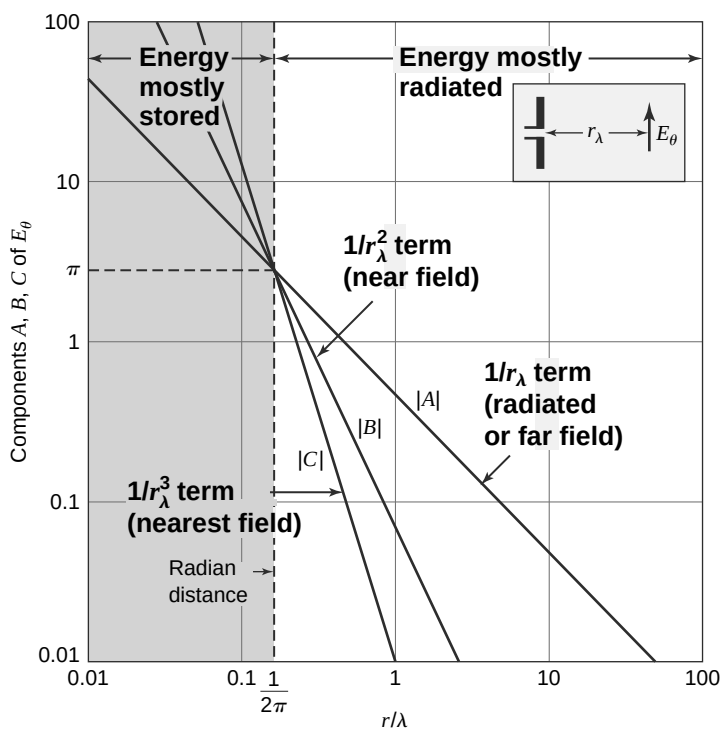

Figure 6–5 Variation of the magnitudes of the components of E_θ of a short electric dipole as a function of distance (r/λ). The magnitudes of all components equal π at the radian distance $1/(2\pi)$. At larger distances energy is mostly radiated, at smaller distances mostly stored.

For the special case where $\theta = 90°$ (perpendicular to the dipole in the xy plane of Fig. 6–2) and at $r_\lambda \gg 1/(2\pi)$,

$$|H_\phi| = \frac{I_0 L_\lambda}{2r} \qquad (\text{A m}^{-1}) \tag{29}$$

while at $r_\lambda \ll 1/(2\pi)$,

$$|H_\phi| = \frac{I_0 L}{4\pi r^2} \tag{30}$$

which is identical to the relation for the magnetic field perpendicular to a short linear conductor carrying direct current as given by (28).

The magnetic field *at any distance r* from an infinite linear conductor with direct current is given by

$$H_\phi = \frac{I_0}{2\pi r} \tag{31}$$

which is *Ampere's law*.

Remarkably, the magnitude of the magnetic field in the equatorial plane ($\theta = 90°$) *in the far field of an oscillating* $\lambda/2$ *dipole* is identical to (31) (Ampere's law). It is assumed that the current distribution on the $\lambda/2$ dipole is sinusoidal. This is discussed in more detail in Sec. 6–5.

Rearranging the three field components of Table 6–1 for a short electric dipole, we have

$$E_r = \frac{[I]L_\lambda Z \cos\theta}{\lambda}\left[\frac{1}{2\pi r_\lambda^2} - j\frac{1}{4\pi^2 r_\lambda^3}\right] \tag{32}$$

$$E_\theta = \frac{[I]L_\lambda Z \sin\theta}{\lambda}\left[j\frac{1}{2r_\lambda} + \frac{1}{4\pi r_\lambda^2} - j\frac{1}{8\pi^2 r_\lambda^3}\right] \tag{33}$$

$$H_\phi = \frac{[I]L_\lambda \sin\theta}{\lambda}\left[j\frac{1}{2r_\lambda} + \frac{1}{4\pi r_\lambda^2}\right] \tag{34}$$

We note that the constant factor in each of the terms in brackets differs from the factors of adjacent terms by a factor of 2π.

At *the radian distance* ($r_\lambda = 1/2\pi$) the fields of (32), (33) and (34) reduce to

$$E_r = \frac{2\sqrt{2}\pi[I]L_\lambda Z \cos\theta}{\lambda}\underline{/-45°} \tag{35}$$

$$E_\theta = \frac{\pi[I]L_\lambda Z \sin\theta}{\lambda} \tag{36}$$

$$H_\phi = \frac{\sqrt{2}\pi[I]L_\lambda \sin\theta}{\lambda}\underline{/45°} \tag{37}$$

The magnitude of the *average power flux* or *Poynting vector* in the θ direction is given by

$$S_\theta = \tfrac{1}{2}\,\text{Re}\; E_r H_\phi^* = \tfrac{1}{2}E_r H_\phi\;\text{Re}\; 1\underline{/-90°} = \tfrac{1}{2}E_r H_\phi \cos(-90°) = 0 \tag{38}$$

indicating that *no power is transmitted. However, the product* $E_r H_\phi$ *represents imaginary or reactive energy that oscillates back and forth from electric to magnetic energy twice per cycle.*

In like manner the magnitude of the power flux or Poynting vector in the r direction is given by

$$S_r = \tfrac{1}{2} E_\theta H_\phi \cos(-45°) = \frac{1}{2\sqrt{2}} E_\theta H_\phi \tag{39}$$

indicating *energy flow in the r direction.*

Much closer to the dipole [$r_\lambda \ll 1/(2\pi)$], (32), (33) and (34) reduce approximately to

$$E_r = -j \frac{[I] L_\lambda Z \cos\theta}{4\pi^2 \lambda r_\lambda^3} \tag{40}$$

$$E_\theta = -j \frac{[I] L_\lambda Z \sin\theta}{8\pi^2 \lambda r_\lambda^3} \tag{41}$$

$$H_\phi = \frac{[I] L_\lambda \sin\theta}{4\pi \lambda r_\lambda^2} \tag{42}$$

From these equations it is apparent that $S_r = S_\theta = 0$. However, the products $E_r H_\phi$ and $E_\theta H_\phi$ represent imaginary or reactive energy oscillating back and forth but not going anywhere. Thus, *close to the dipole there is a region of almost complete energy storage.*

Remote from the dipole [$r_\lambda \gg 1/(2\pi)$], (32), (33) and (34) reduce approximately to

$$E_r = 0 \tag{43}$$

$$E_\theta = j \frac{[I] L_\lambda Z \sin\theta}{2\lambda r_\lambda} \tag{44}$$

$$H_\phi = j \frac{[I] L_\lambda \sin\theta}{2\lambda r_\lambda} \tag{45}$$

Since $E_r = 0$, there is no energy flow in the θ direction ($S_\theta = 0$). However, *since $E_\theta H_\phi$ are in time phase, their product represents real power flow in the outward radial direction. This power is radiated.*

Many antennas behave like the dipole with large energy storage close to the antenna.

The region near the dipole is one of stored energy (reactive power) while regions remote from the dipole are ones of radiation. The radian sphere at $r_\lambda = 1/(2\pi)$ marks a zone of transition from one region to the other with a nearly equal division of the imaginary and real (radiated) power.

The region close to the dipole may be likened to a spherical resonator within which pulsating energy is trapped, but with some leakage which is radiated. There is no exact boundary to this resonator region, but if we arbitrarily put it at the radian distance a qualitative picture may be sketched as in Fig. 6–6.

6–4 Radiation Resistance of Short Electric Dipole

Let us now calculate the radiation resistance of the short dipole of Fig. 6–1*b*. This may be done as follows. The Poynting vector of the far field is integrated over a large sphere to obtain the total power radiated. This power is then equated to $I^2 R$ where I is the rms current on the dipole and R is a resistance, called the radiation resistance of the dipole.

The *average* Poynting vector is given by

$$S = \tfrac{1}{2} \mathrm{Re}(E \times H^*) \tag{1}$$

The far-field components are E_θ and H_ϕ so that the radial component of the Poynting vector is

$$S_r = \tfrac{1}{2} \mathrm{Re}\, E_\theta H_\phi^* \tag{2}$$

where E_θ and H_ϕ^* are complex.

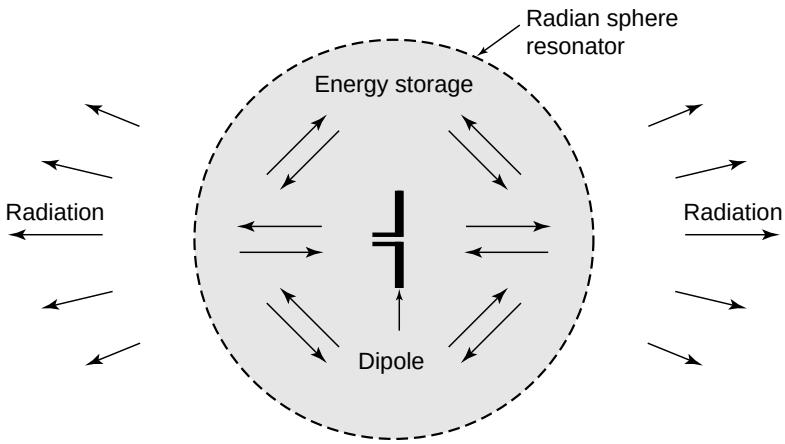

Figure 6–6 Sketch suggesting that within the radian sphere at $r = \lambda/2\pi = 0.16\lambda$ the situation is like that inside a resonator with high-density pulsating energy accompanied by leakage which is radiated.

The far-field components are related by the intrinsic impedance of the medium. Hence,

$$E_\theta = H_\phi Z = H_\phi \sqrt{\frac{\mu}{\varepsilon}} \tag{3}$$

Thus, (2) becomes

$$S_r = \tfrac{1}{2} \operatorname{Re} Z H_\phi H_\phi^* = \tfrac{1}{2} |H_\phi|^2 \operatorname{Re} Z = \tfrac{1}{2} |H_\phi|^2 \sqrt{\frac{\mu}{\varepsilon}} \tag{4}$$

The total power P radiated is then

$$P = \iint S_r \, ds = \frac{1}{2} \sqrt{\frac{\mu}{\varepsilon}} \int_0^{2\pi} \int_0^{\pi} |H_\phi|^2 r^2 \sin\theta \, d\theta \, d\phi \tag{5}$$

where the angles are as shown in Fig. 6–2 and $|H_\phi|$ is the absolute value of the magnetic field, which from (6–3–18) is

$$|H_\phi| = \frac{\omega I_0 L \sin\theta}{4\pi c r} \tag{6}$$

Substituting this into (5), we have

$$P = \frac{1}{32} \sqrt{\frac{\mu}{\varepsilon}} \frac{\beta^2 I_0^2 L^2}{\pi^2} \int_0^{2\pi} \int_0^{\pi} \sin^3\theta \, d\theta \, d\phi \tag{7}$$

The double integral equals $8\pi/3$ and (7) becomes

$$P = \sqrt{\frac{\mu}{\varepsilon}} \frac{\beta^2 I_0^2 L^2}{12\pi} \tag{8}$$

This is the *average* power or rate at which energy is streaming out of a sphere surrounding the dipole. Hence, it is equal to the power radiated. Assuming no losses, it is also equal to the power delivered to the dipole.

Therefore, P must be equal to the square of the rms current I flowing on the dipole times a resistance R_r called the *radiation resistance* of the dipole. Thus,

$$\sqrt{\frac{\mu}{\varepsilon}}\frac{\beta^2 I_0^2 L^2}{12\pi} = \left(\frac{I_0}{\sqrt{2}}\right)^2 R_r \tag{9}$$

Solving for R_r,

$$R_r = \sqrt{\frac{\mu}{\varepsilon}}\frac{\beta^2 L^2}{6\pi} \tag{10}$$

For air or vacuum $\sqrt{\mu/\varepsilon} = \sqrt{\mu_0/\varepsilon_0} = 377 = 120\pi\,\Omega$ so that (10) becomes[1]

Dipole with uniform current $$R_r = 80\pi^2\left(\frac{L}{\lambda}\right)^2 = 80\pi^2 L_\lambda^2 = 790 L_\lambda^2 \quad (\Omega)$$ ***Radiation resistance*** (11)

As an example suppose that $L_\lambda = \frac{1}{10}$. Then $R_r = 7.9\ \Omega$. If $L_\lambda = 0.01$, then $R_r = 0.08\ \Omega$. Thus, the radiation resistance of a short dipole is small.

In developing the field expressions for the short dipole, which were used in obtaining (11), the restriction was made that $\lambda \gg L$. This made it possible to neglect the phase difference of field contributions from different parts of the dipole. If $L_\lambda = \frac{1}{2}$ we violate this assumption, but, as a matter of interest, let us find what the radiation resistance of a $\lambda/2$ dipole is, when calculated in this way. Then for $L_\lambda = \frac{1}{2}$, we obtain $R_r = 197\ \Omega$. The correct value is 168 Ω (see Prob. 6–6–1), which indicates the magnitude of the error introduced by violating the restriction that $\lambda \gg L$ to the extent of taking $L = \lambda/2$.

It has been assumed that with end loading (see Fig. 6–1*a*) the dipole current is uniform. However, with no end loading the current must be zero at the ends and, if the dipole is short, the current tapers almost linearly from a maximum at the center to zero at the ends, as in Fig. 2–12, with an average value of $\frac{1}{2}$ of the maximum. Modifying (8) for the general case where the current is not uniform on the dipole, the *radiated power* is

$$P = \sqrt{\frac{\mu}{\varepsilon}}\frac{\beta^2 I_{\text{av}}^2 L^2}{12\pi} \qquad \text{(W)} \tag{12}$$

where I_{av} = amplitude of *average current* on dipole (peak value in time)

The *power delivered* to the dipole is, as before,

$$P = \tfrac{1}{2} I_0^2 R_r \qquad \text{(W)} \tag{13}$$

where I_0 = amplitude of *terminal current* of center-fed dipole (peak value in time). Equating the *power radiated* (12) to the *power delivered* (13) yields, for free space ($\mu = \mu_0$ and $\varepsilon = \varepsilon_0$), a radiation resistance

$$R_r = 790\left(\frac{I_{\text{av}}}{I_0}\right)^2 L_\lambda^2 \qquad (\Omega) \tag{14}$$[2]

[1] $\sqrt{\mu_0/\varepsilon_0} = 376.73\ \Omega$. 377 and 120π are convenient approximations.

[2] As already given by (2–10–9).

For a short dipole without end loading, we have $I_{\text{av}} = \frac{1}{2} I_0$, as noted above, and (14) becomes

$$R_r = 197 L_\lambda^2 \qquad (\Omega) \tag{15}$$

6–5 The Thin Linear Antenna

In this section expressions for the far-field patterns of thin linear antennas will be developed. It is assumed that the antennas are symmetrically fed at the center by a balanced two-wire transmission line. The antennas may be of any length, but it is assumed that the current distribution is sinusoidal. Current-distribution measurements indicate that this is a good assumption provided that the antenna is thin, i.e., when the conductor diameter is less than, say, $\lambda/100$. Thus, the sinusoidal current distribution approximates the natural distribution on thin antennas. Examples of the approximate natural-current distributions on a number of thin, linear center-fed antennas of different length are illustrated in Fig. 6–7. The currents are in phase over each $\lambda/2$ section and in opposite phase over the next.

Referring to Fig. 6–8, let us now proceed to develop the far-field equations for a symmetrical, thin, linear, center-fed antenna of length L. The retarded value of the current at any point z on the antenna referred to a point at a distance s is

$$[I] = I_0 \sin\left[\frac{2\pi}{\lambda}\left(\frac{L}{2} \pm z\right)\right] e^{j\omega[t-(r/c)]} \tag{1}$$

In (1) the function

$$\sin\left[\frac{2\pi}{\lambda}\left(\frac{L}{2} \pm z\right)\right]$$

is the form factor for the current on the antenna. The expression $(L/2) + z$ is used when $z < 0$ and $(L/2) - z$ is used when $z > 0$. By regarding the antenna as made up of a series of infinitesimal dipoles of length dz, the field of the entire antenna may then be obtained by integrating the fields from all of the dipoles making up the antenna with the result[1]

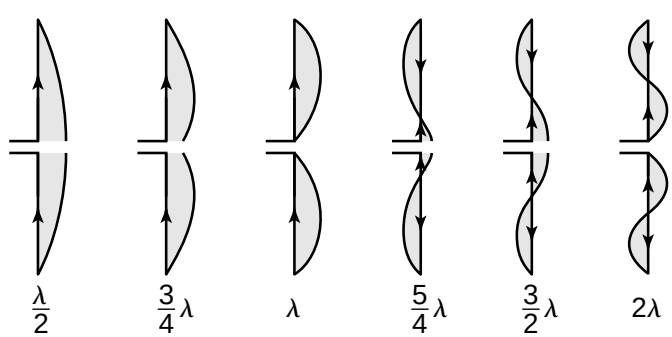

Figure 6–7 Approximate natural-current distribution for thin, linear, center-fed antennas of various lengths.

[1]For complete development, see the second edition of this book, pp. 220–221.

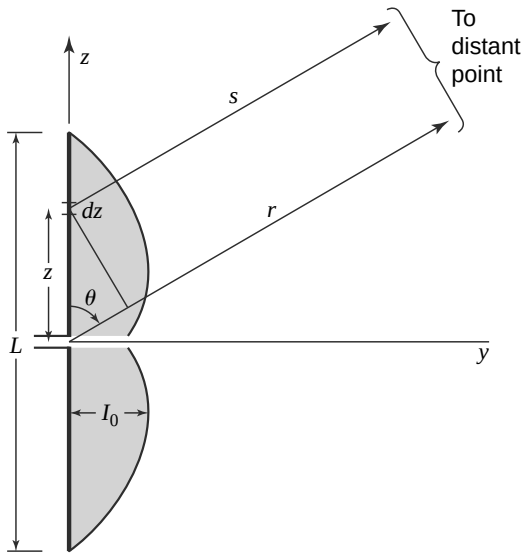

Figure 6–8 Relations for symmetrical, thin, linear, center-fed antenna of length L.

Far fields of center-fed dipole

$$H_\phi = \frac{j[I_0]}{2\pi r}\left[\frac{\cos[(\beta L\cos\theta)/2] - \cos(\beta L/2)}{\sin\theta}\right] \tag{2}$$

$$E_\theta = \frac{j60[I_0]}{r}\left[\frac{\cos[(\beta L\cos\theta)/2] - \cos(\beta L/2)}{\sin\theta}\right] \tag{3}$$

where $[I_0] = I_0 e^{j\omega[t-(r/c)]}$ and

$$E_\theta = 120\pi H_\phi \tag{3a}$$

Equations (2), (3) and (3*a*) give the far fields H_ϕ and E_θ of a *symmetrical, center-fed, thin linear antenna of length L*. The shape of the far-field pattern is given by the factor in the brackets. The factors preceding the brackets in (2) and (3) give the instantaneous magnitude of the fields as functions of the antenna current and the distance r. To obtain the rms value of the field, we let $[I_0]$ equal the rms current at the location of the current maximum. There is no factor involving phase in (2) or (3), since the center of the antenna is taken as the phase center. Hence any phase change of the fields as a function of θ will be a jump of 180° when the pattern factor changes sign.

As examples of the far-field patterns of linear center-fed antennas, three antennas of different lengths will be considered. Since the amplitude factor is independent of the length, only the relative field patterns as given by the pattern factor will be compared.

EXAMPLE 6–5.1 $\lambda/2$ Antenna

When $L = \lambda/2$, the pattern factor becomes

$$E = \frac{\cos[(\pi/2)\cos\theta]}{\sin\theta} \tag{4}$$

This pattern is shown in Fig. 6–9*a*. It is only slightly more directional than the pattern of an infinitesimal or short dipole which is given by $\sin\theta$. The beamwidth between half-power points of the $\lambda/2$ antenna is 78° as compared to 90° for the short dipole.

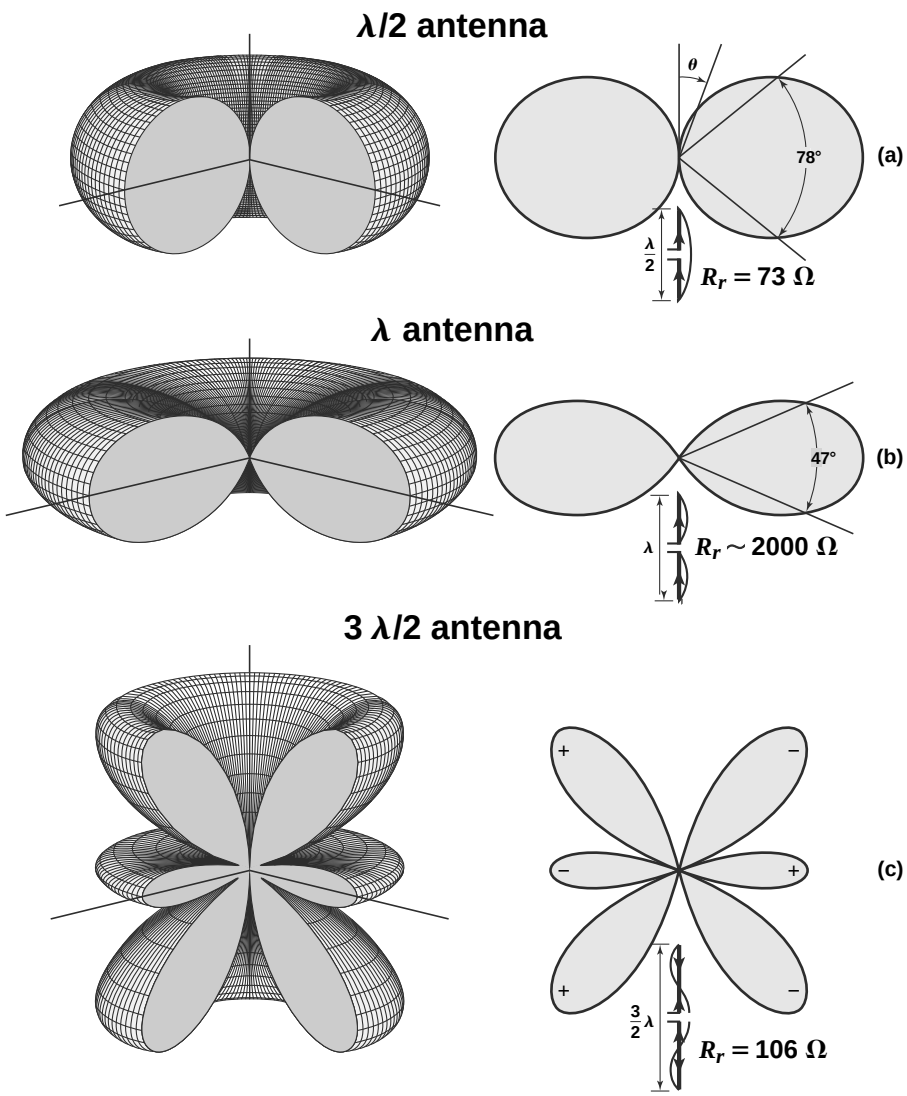

Figure 6–9 Three-dimensional and polar plots of the patterns of $\lambda/2$, λ, and 3 $\lambda/2$ antennas. The antennas are center-fed with current distributions assumed sinusoidal as indicated.

EXAMPLE 6–5.2 Full-Wave (λ) Antenna

When $L = \lambda$, the pattern factor becomes

$$E = \frac{\cos(\pi \cos\theta) + 1}{\sin\theta} \tag{5}$$

This pattern is shown in Fig. 6–9*b*. The half-power beamwidth is 47°.

EXAMPLE 6–5.3 Three Half-Wave ($3\lambda/2$) Antenna

When $L = 3\,\lambda/2$, the pattern factor is

$$E = \frac{\cos\left(\frac{3}{2}\pi \cos\theta\right)}{\sin\theta} \tag{6}$$

The pattern for this case is presented in Fig. 6–9*c*. With the midpoint of the antenna as phase center, the phase shifts 180° at each null, the relative phase of the lobes being indicated by the + and − signs. In all three cases, (*a*), (*b*) and (*c*), the space pattern is a figure-of-revolution of pattern shown around the axis of the antenna.

EXAMPLE 6–5.4 Field at Any Distance from Center-Fed Dipole

The geometry for the field at the point P from a symmetrical center-fed dipole of length L with sinusoidal current distribution is presented in Fig. 6–10. The maximum current is I_0. It may be shown that the z component of the electric field at the point P is given by

$$E_z = \frac{-jI_0Z}{4\pi}\left[\frac{e^{-j\beta s_1}}{s_1} + \frac{e^{-j\beta s_2}}{s_2} - 2\cos\frac{\beta L}{2}\frac{e^{-j\beta r}}{r}\right] \tag{7}$$

The ϕ component of the magnetic field at the point P (Fig. 6–10) is given by

$$H_\phi = \frac{jI_0}{4\pi r\sin\theta}\left(e^{-j\beta s_1} + e^{-j\beta s_2} - 2\cos\frac{\beta L}{2}e^{-j\beta r}\right) \tag{8}$$

Whereas the other field equations for oscillating dipoles given in this chapter apply only with the restrictions of $\lambda \gg L$ and $r \gg L$, (7) and (8) apply without distance restrictions.

If P lies on the y axis ($\theta = 90°$) and the dipole is $\lambda/2$ long, (7) becomes

$$E_z = \frac{I_0Z}{2\pi\lambda\sqrt{\frac{1}{16} + r_\lambda^2}} \angle\left(-360°\sqrt{\frac{1}{16} + r_\lambda^2} - 90°\right) \quad (\text{V m}^{-1}) \tag{9}$$

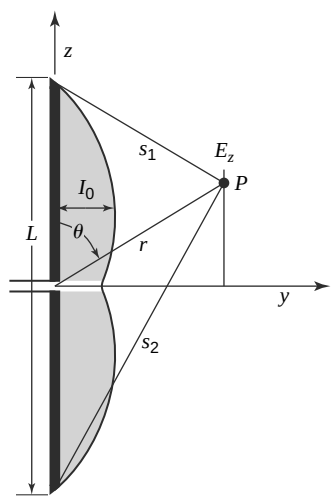

Figure 6–10 Symmetrical center-fed dipole with sinusoidal current distribution. The field component E_z at any distance can be expressed as the sum of three components radiating from the ends and the center of the dipole.

and (8) becomes

$$H_\phi = \frac{I_0}{2\pi r} \angle -360^\circ \sqrt{\frac{1}{16} + r_\lambda^2} + 90^\circ \qquad (\text{A m}^{-1}) \tag{10}$$

where

$r_\lambda = r/\lambda$
$Z = 377\ \Omega$
$I_0 =$ maximum current $=$ terminal current

At a large distance the ratio of E_z as given by (9) to H_ϕ as given by (10) is

$$\frac{E_z}{H_\phi} = Z = 377\ \Omega = \text{intrinsic impedance (resistance) of space} \tag{11}$$

The magnitude of H_ϕ is

$$|H_\phi| = \frac{I_0}{2\pi r} \qquad (\text{A m}^{-1}) \tag{12}$$

6–6 Radiation Resistance of λ/2 Antenna

To find the radiation resistance, the Poynting vector is integrated over a large sphere yielding the power radiated, and this power is then equated to $(I_0/\sqrt{2})^2 R_0$, where R_0 is the radiation resistance at a current maximum point and I_0 is the peak value in time of the current at this point. The total power P radiated was given in (6–4–5)[1] in terms of H_ϕ for a short dipole. In (6–4–5), $|H_\phi|$ is the absolute value. Hence, the corresponding value of H_ϕ for a linear antenna is obtained from (6–5–2) by putting $|j[I_0]| = I_0$. Substituting this into 6–4–5, we obtain

$$P = \frac{15 I_0^2}{\pi} \int_0^{2\pi} \int_0^{\pi} \frac{\{\cos[(\beta L/2)\cos\theta] - \cos(\beta L/2)\}^2}{\sin\theta}\, d\theta\, d\phi \tag{1}$$

$$= 30 I_0^2 \int_0^{\pi} \frac{\{\cos[(\beta L/2)\cos\theta] - \cos(\beta L/2)\}^2}{\sin\theta}\, d\theta \tag{2}$$

Equating the radiated power as given by (2) to $I_0^2 R_0/2$ we have

$$P = \frac{I_0^2 R_0}{2} \tag{3}$$

and

$$R_0 = 60 \int_0^{\pi} \frac{\{\cos[(\beta L/2)\cos\theta] - \cos(\beta L/2)\}^2}{\sin\theta}\, d\theta \tag{4}$$

where the radiation resistance R_0 is referred to the current maximum. In the case of a $\lambda/2$ antenna this is at the center of the antenna or at the terminals of the transmission line (see Fig. 6–7).

[1] $P = \iint S \cdot ds = \frac{1}{2}\sqrt{\mu/\varepsilon} \iint |H_\phi|^2\, ds$

Proceeding with the evaluation of (4) with the aid of the sine integral, $\text{Si}(x)$, and the cosine integral, $\text{Cin}(x)$, it may be shown that the radiation resistance of the $\lambda/2$ antenna is

$$R_r = 30\ \text{Cin}(2\pi) = 30 \times 2.44 = \mathbf{73\ \Omega} \tag{5}$$

This is the well-known value for the radiation resistance of a thin, linear, center-fed, $\lambda/2$ antenna with sinusoidal current distribution. The terminal impedance also includes some inductive reactance as discussed in Chap. 18. That is,

$$Z = 73 + j42.5\ \Omega \tag{6}$$

To make the reactance zero, that is, to make the antenna resonant, requires that the antenna be shorted a few percent less than $\lambda/2$. This shortening also results in a reduction in the value of the radiation resistance to about 65 Ω.

6–7 Radiation Resistance at a Point Which is not a Current Maximum

If we calculate, for example, the radiation resistance of a $3\lambda/4$ antenna (see Fig. 6–7) by the above method, we obtain its value at a current maximum. This is not the point at which the transmission line is connected. Neglecting antenna losses, the value of radiation resistance so obtained is the resistance R_0 which would appear at the terminals of a transmission line connected at a current maximum in the antenna, *provided* that the current distribution on the antenna is the same as when it is center-fed as in Fig. 6–7. Since a change of the feed point from the center of the antenna may change the current distribution, the radiation resistance R_0 is not the value which would be measured on a $3\lambda/4$ antenna or on any symmetrical antenna whose length is not an odd number of $\lambda/2$. However, R_0 can be easily transformed to the value which would appear across the terminals of the transmission line connected at the center of the antenna.

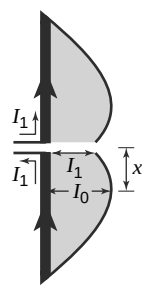

Figure 6–11 Relation of current I_1 at transmission-line terminals to current I_0 at current maximum.

This may be done by equating (6–6–3) to the power supplied by the transmission line, given by $I_1^2 R_1/2$, where I_1 is the current amplitude at the terminals and R_1 is the radiation resistance at this point (see Fig. 6–11). Thus,

$$\frac{I_1^2}{2} R_1 = \frac{I_0^2}{2} R_0 \tag{1}$$

where R_0 is the radiation resistance calculated at the current maximum. Thus, the radiation resistance appearing at the terminals is

$$R_1 = \left(\frac{I_0}{I_1}\right)^2 R_0 \tag{2}$$

The current I_1 at a distance x from the nearest current maximum, as shown in Fig. 6–11, is given by

$$I_1 = I_0 \cos \beta x \tag{3}$$

where

I_1 = terminal current
I_0 = maximum current